2008

Directed self-assembly of gold nanorods using surface modification

David A. Walker
University of South Florida

Directed Self-Assembly of Gold Nanorods Using Surface Modification

by

David A. Walker

A thesis submitted in partial fulfillment
of the requirements for the degree of
Master of Science in Chemical Engineering
Department of Chemical & Biomedical Engineering
University of South Florida

Major Professor: Vinay, K. Gupta, Ph.D.
Ryan G. Toomey, Ph.D.
Daniel H. Yeh, Ph.D.

Date of Approval:
July 10, 2008

Keywords: poly(L-glutamic acid), resorcinarene, monolayers, composite particles, linear assembly, end-to-end assembly, reversible assembly, nanotechnology, sensors, metallic nanoparticles

DEDICATION

This thesis is dedicated to my parents and my little brother.

Dale F. Walker

Alan W. Walker

Nathan F. Walker

It is through their unconditional love, continued understanding and unwavering support that I have been able to complete this work.

This thesis is dedicated to my past professors and teachers. It is through their experience that they have imparted me with knowledge. It is through their enthusiasm for teaching that they have imparted me with inspiration.

This thesis is dedicated to you. It is through you that the knowledge contained in this work will be remembered.

With Love,

David

ACKNOWLEGEMENTS

First, I would like to thank my advisor and mentor, Dr. Vinay K. Gupta, who has provided me with an invaluable learning experience over the past two and a half years. It is because of Dr. Gupta's continued diligence and support that I have had a gratifying graduate career. I will always appreciate the time he took to train me and to enhance my knowledge and understanding on a wide array of topics vital to the success of my graduate studies. I would also like to thank my committee members, Dr. Ryan Toomey and Dr. Daniel Yeh, who have played an integral part in my graduate education. I would like to show appreciation all of the professors in the department which have taught me a great deal over the past four years. A special thanks to my lab partners who served as my family at my home away from home (the lab): Mr. Cecil Coutinho, Ms. Dayling Chaparro, Mr. Adrian P. Defante, Ms. Justine Molas, Mr. Bijith Mankidy, Dr. Jeung-Yeop Shim, Ms. Chhavi Manocha, Ms. Fedena Fanord, and Ms. Reshma Harrinauth. I would also like to thank Mr. Cecil Coutinho for mentoring me in the lab as an undergraduate and for becoming a close friend. I would like to thank Dr. Shim for his initial work on the synthesis of gold nanorods and to Dr. Alveda Williams for the synthesis of the polypeptide used in this work. I would also like to thank the NSF STARS program (NSF Award 0638709) which provided me with the financial support to pursue my graduate education.

TABLE OF CONTENTS

LIST OF FIGURES

Directed Self-Assembly of Gold Nanorods Using Surface Modification

David A. Walker

ABSTRACT

Metallic nanoparticles are unique materials for optical, electronic, catalytic, and sensing applications. Due to the vast flexibility in controlling the surface chemistry of these particles through functionalization there is a great deal of interest in using metallic nanoparticles as building blocks in the development of more complex nanostructures through the use of a 'bottom-up' approach. Using self assembly techniques, one can exploit spontaneous chemical interactions to build complex constructs on the nanometer scale.

Towards this end, gold nanorods have been synthesized and modified with various polymers, inorganic oxides and organic ligands to establish principles for self-assembly of these unique nanomaterials. Gold nanorods are of great interest due to their strong optical absorption in the visible and near infrared regions, which can be tuned through material preparation and modification of the surrounding environment. This thesis focuses on investigating approaches for both irreversible and reversible self-assembly of gold nanorods. Techniques such as dynamic light scattering (DLS), ultraviolet-visible (UV) spectroscopy, transmission electron microscopy (TEM), and polarization modulation infrared

reflection absorbance spectroscopy (PM-IRRAS) were used to characterize the colloidal particles and gold surfaces. A novel contribution of this work is the successful demonstration of end-to-end linking of gold nanorods in a rapid and reversible manner using a pH responsive polypeptide.

CHAPTER ONE: INTRODUCTION, MOTIVATION AND BACKGROUND

1.1 Introduction to Gold Nanorods

Metallic nanoparticles are unique materials with a wide array of applications in the fields of optics, electronics, catalysis, and sensors[1-5]. Due to recent advances in controlling the surface chemistry of these particles through functionalization there is a great deal of interest in using metallic nanoparticles as building blocks in the development of more complex nanostructures through the use of a 'bottom-up' approach[3, 5-15].

Increasingly, gold nanorods have gained attention due to their strong optical absorption in the visible and near infrared regions which can be tuned either during the synthesis of the nanorod or after synthesis by modification of the particle or its surrounding environment[16-24]. These anisotropic particles have already shown great promise in the development of new biological detection and sensor devices[14, 25-30]. Gold nanorods are also being investigated for applications as nanoscale wave guides to carry electromagnetic signals through a chain of particles[31, 32]. Yet, the controlled self-assembly of these particles into ordered structures is still a limiting factor in many applications[33].

The broad aim of this thesis is to direct the irreversible and reversible assembly of gold nanorods by various techniques that rely on surface

functionalization. The following sections will provide an introduction to the synthesis of gold nanorods as well as the various assembly and functionalization techniques which are essential to this research. Chapter One will conclude with a description of the aims and objectives of this thesis.

1.1.1 Optical Properties

One of the most well known and commonly utilized property of gold nanorods is their unique optical absorbance in the visible and the near infrared region[4, 16, 21, 23, 34]. The absorbance spectrum of colloidal gold nanorods, as shown in Figure 1.1, contains two distinct peaks correlating to the two optical resonances of the nanorod. One of the two peaks can be identified at approximately 500 nm and corresponds to the transverse surface plasmon resonance of the nanorod. This peak is the same as the transverse resonance of spherical gold nanoparticles that is responsible for the distinct red coloration of solutions of colloidal gold particles[21, 34].

Surface modifications of the gold nanorods and nanoparticles can typically lead to shifts in the transverse resonance. A red-shift in the resonance is indicative of coatings by materials that result in an increase in the local refractive index of the medium surrounding the nanoparticle[35, 36]. The magnitude of the shift in the transverse resonance is related to the thickness of the coating that has been applied to the particle, with a thin coating resulting in a smaller shifts in the resonance[18, 35, 36].

The second and more prominent peak in the spectrum of gold nanorods in Figure 1.1 is attributed to the longitudinal surface plasmon resonance of the nanorod. The location of this peak is dependent on the aspect ratio of the nanorod. By controlling the reaction conditions during synthesis, the aspect ratio, and thereby the location of the longitudinal resonance, can be tuned to a desired wavelength[20, 21, 24, 37]. The longitudinal resonance of the rods can also be altered post synthesis through the addition of coatings or through functionalization as is the case for the transverse resonance.

In contrast to optical absorption, the fluorescence of gold nanorods has only been investigated in greater detail in recent years[38-40], following the development of techniques to control the assembly of these particles. Fluorescence is a phenomena where photons are absorbed by a material at a given energy state followed by the emission of photons at a lower energy state as shown in Figure 1.2. While the final effect of emitting photons at a lower energy state than the incident photons is similar to the phenomenon of Raman scattering, the two optical phenomena differ in that fluorescence occurs only for specific frequencies of incident photons, while Raman scattering can occur for any frequency of incident photons. In order to describe the efficiency of the fluorescence of a material, a value referred to as the quantum efficiency or the quantum yield is used. The quantum yield is a ratio between the number of photons emitted by a material to the number of photons which were originally absorbed.

In the case of short gold nanorods with low aspect ratios, as used in this research, it has been shown through both theoretical calculations and experimentation that quantum yields are low i.e. the fluorescence is weak[40]. It has also been shown that for longer gold nanorods with higher aspect ratios, the quantum yield increases substantially, thereby, widening the uses and applications of gold nanorods as fluorescent markers[39].

When gold nanorods fluoresce, two emission bands are found, corresponding to the transverse and longitudinal plasmon resonances[39]. Reports have shown that these fluorescent bands fall between 500 nm and 800 nm and are dependent on the length of the gold nanorods, the aspect ratio of the gold nanorods, as well as the frequency of the incident photons[38-40].

One of the most promising applications in this context is the use of gold nanorods as fluorescent markers for biomolecules and DNA. Current fluorescent labels used for tagging DNA in microarray analysis are expensive and extremely photosensitive, which requires special care when working with the chemical labels. Gold nanorods modified with complimentary strands of thiolated DNA provide a simple and inexpensive alternative to the chemical fluorescent labels[39].

Recently, it has been shown that gold nanorods produce the optical phenomena known as hyper-Rayleigh scattering (HRS)[26, 41]. Light scattering techniques are well-known to be useful in determining the various properties of small colloidal particles. Rayleigh scattering is a common phenomenon where photons are scattered by particles much smaller than the wavelength of incident light at an equivalent frequency to the incident photons. In hyper-Rayleigh

scattering light is scattered by small particles, similar to Rayleigh scattering, but due to the high polarizability of the particle the frequency of the scattered photons is exactly twice that of the incident photons[41] as depicted in Figure 1.2.

HRS spectroscopy of gold nanorods has been used to detect the presence of the HIV virus at picomolar concentrations[26]. In this novel design, gold nanorods modified with strands of fluorescently tagged DNA cause the gold nanorods to aggregate in the presence of DNA from the HIV virus. This aggregation causes a significant change in the HRS of the particles allowing for the detection of the virus. Using similar techniques, HRS of gold nanorods could be exploited to detect extremely low concentrations of other complex organic molecules.

1.1.2 Synthesis Techniques

Over the years, multiple techniques have been developed for the synthesis of gold nanorods. Advances and developments in the synthesis techniques is resulting in reduced complexity of systems based on gold nanorods that can be prepared with high efficiency and reproducibility. A brief summary of several synthetic procedures is provided in this section.

The template method was first developed by Martin and co-workers[42-44]. In this method, gold is electrochemically deposited within the pores of either a polycarbonate or alumina template membrane. Initially, a conductive layer of material is deposited on one side of the template membrane. This conductive support is then used to drive the electro-deposition of gold from the opposing

side of the membrane. After the gold has filled the pores of the template membrane, a chemical additive is used to dissolve and remove the template. The gold nanorods which are left behind on the conductive support can then be stabilized with polymers before the conductive support is dissolved to release the gold nanorods and create a colloidal suspension[45]. Figure 1.3 shows a step-by-step schematic depicting this process. In this technique the diameter of the rod is governed by the diameter of the pore of the template membrane. The length of the rod can be controlled by the amount of gold deposited into the pores of the membrane[46]. While it is easy to tune the final dimensions of the gold nanorods using this technique, the yield of the gold nanorods is extremely low because they are produced one monolayer at a time.

In the electrochemical method of synthesizing gold nanorods, first publicized by Wang and co-workers[23, 47], an electrical potential is placed across a gold anode and a platinum cathode. The two electrodes are placed in an electrolytic solution containing cationic surfactants which form cylindrical micelles[48]. As gold ions from the anode are deposited onto the platinum cathode, the surfactant stabilizes the rod allowing it to grow in a cylindrical manner. The exact mechanism is unknown but it is believed that the gold nanorods grow on the surface of the platinum cathode. The nanorods are stabilized by the surfactant micelles that form around them and then detach from the cathode at a critical length when sonicated. It was found by Wang and co-workers that the presence of silver ions, introduced through the addition of a silver plate has a large effect on the yield of the gold nanorods as well as on the

final aspect ratio of the rods. A simplified schematic of the required set-up is depicted in Figure 1.4, while a more detailed schematic of the formation of the gold nanorods on the platinum cathode is shown in Figure 1.5.

The seed mediated method was first implemented by Nathan and co-workers when solutions containing 4-5% gold nanorods were produced[49]. These techniques have been advanced and refined by Jana in collaboration with C.J. Murphy and co-workers into the present-day seed mediated techniques[19-21]. The seed mediated method utilizes gold nanoparticles as seeds that are placed in a growth solution containing surfactants, gold ions, silver ions, and a weak reducing agent. The seeds act as a point of nucleation for the continued growth of the particle as the metallic surface of the seed is necessary for the weak reducing agent to reduce the gold ions in the solution. Surfactants present in the growth solution form a bi-layer and help to direct the growth of the nanoparticles in a cylindrical fashion. While the exact mechanism is not yet fully understood, it is believed to operate as a 'zipper' mechanism[17]. In this mechanism the gold nanorod grows while the surfactant immediately assembles along certain crystalline facets preventing growth in that direction[50]. A schematic of the 'zipper' mechanism can be seen in Figure 1.6.

In the seed mediated method it is common to use gold nanorods formed in the first growth solution as seeds in a new growth solution. When the gold nanorod seeds are placed in the new growth solution, the nanorods continue to grow in length[17]. While this technique can be used to control the length of the gold nanorods during synthesis, the yield of nanorods decreases with each

subsequent growth solution as the number of seed particles is reduced. Figure 1.7 depicts a typical seed mediated growth procedure.

1.1.3 Controlling the Properties of Gold Nanorods

The main property of gold nanorods that can be controlled during synthesis is their aspect ratio. In the case of the template based method, this is easily done by the selection of the membrane to control the diameter of the particle and the thickness of gold to be deposited for control over the length of the rod[46, 51]. In the case of the electrochemical method, it has been shown that the concentration of the silver ions in the reaction cell plays a role in determining the final aspect ratio of the gold nanorods[23], but the exact mechanism of how this is accomplished is still unknown.

In the seed mediated method it has been shown that many factors can affect the final aspect ratio. First, the formulation of the growth solution plays a large role. By changing the ratio of gold nanoparticle seeds with the concentration of gold ions in the growth solution the final length of rod can be tuned[17]. By decreasing the number of gold seeds, the number of gold ions per particle will increase, allowing for the nanorods to grow longer. The drawback in reducing the number of seed particles is that the yield of gold nanorods that will be produced will also decrease.

The concentration of silver ions has also been shown to affect the final aspect ratio and yield of gold nanorods[22, 24]. By introducing silver ions, the yield of gold nanorods increases significantly while also effecting the final aspect ratio

of the nanorods. It has been shown that upon exceeding a critical concentration of silver ions, the presence of excess silver actually retards the growth of gold nanorods. Therefore, it is of great importance to control the concentration of silver in the growth solution of the nanorods in order to influence both the final yield and aspect ratio of the nanorods. The temperature at which the growth solution is maintained during the synthesis has also been shown to have an affect on the aspect ratio of the synthesized nanorods[24]. By increasing the temperature of the growth solution, lower aspect ratio nanorods can be synthesized.

Figure 1.8 depicts the UV-Vis-NIR spectra of several different gold nanorod solutions with differing aspect ratios that have been prepared in this thesis. By fitting the longitudinal peak using theoretical calculations, the distribution of the aspect ratio of the gold nanorods and its average value can be estimated.

Following synthesis, gold nanorods can either be coated or end-functionalized that greatly expands their potential applications. In coating procedures, electrostatic interactions are typically utilized to deposit layers of polyelectrolytes[18, 52] which assist in the stabilization of the gold nanorod. Modification of gold nanorods with polymer layers has also been utilized in depositing gold nanorods onto surfaces through electrostatic interactions. The transverse and longitudinal optical resonances of the gold nanorods are particularly sensitive to changes in the refractive index surrounding the particles and show significant changes when the organic coatings are applied[16, 35, 36, 53].

Another strategy for functionalization of gold nanorods relies on the well-known strong chemical and physical interactions of organosulfides, such as thiols and disulfides, with gold surfaces and particularly <111> facets of gold[54-56]. In the case of gold nanorods, these <111> facets can be located on the ends of the rod where the layers of surfactant and other stabilizing agents are thin and disturbed[20, 21, 57-63]. This combination of factors causes the sulfide functional groups to target and bind specifically near the ends of the gold nanorods. Since there is a wide array of molecules which can be modified with organosulfides, changing the surface chemistry at the ends of the gold nanorod is as simple as selecting an appropriate organosulfide and allowing the molecules to form a self-assembled monolayer on the end of the gold nanorod.

1. 2 Applications of Gold Nanorods

Due to the optical and chemical properties that gold nanorods posses, various applications in biological tagging and imaging[25, 34, 39, 64], sensors[26, 28, 30, 39, 57, 58], nanoelectronics[10, 65], optics and photonics[11, 31, 32, 53, 66], as well as catalysis[67, 68] have been proposed.

Numerous biological tagging or imaging devices have been devised which exploit the optical properties of gold nanorods. Gold nanorods have been used in two methodologies to tag and identify cancer cells. By functionalizing the gold nanorods with complimentary antigens, cancer cells have been detected through the use of photoacoustic imaging[25] which exploits the distinct longitudinal resonance of gold nanorods in the near infrared region. The fluorescence of gold

nanorods with higher aspect ratios has also been employed as a method for the detection of cancerous cells[64]. Several groups that have tagged cancer cells with gold nanorods have proceeded to thermally destroy the cells through the excitement of the longitudinal resonance[69-71]. Continued research in these fields could one day lead to the early detection of many deleterious biological agents in the human body as well as targeted non-invasive forms of treatment.

Several sensor devices have also been developed that employ the optical properties of gold nanorods. Sensors that focus on either the aggregation or assembly of gold nanorods and result in a vivid color change upon detection of an analyte have been developed for the detection of both biological and organic molecules[26, 27, 29, 30, 34, 57, 58]. Also, the ability to detect inorganic molecules[28] by perceivable visual changes in the aspect ratio of the gold nanorods has been developed.

Initial work in applying gold nanorods for nanoelectronics and optics has also shown a great deal of promise. In nanoelectronics, gold nanorods have been proven useful as nanowires in nanocircuits[10, 65]. Beyond applications in nanocircuitry, gold nanorods also have uses in electronic visual displays due to their absorbance in the visible region. In various cases, gold nanorods and other metallic nanoparticles have been embedded into polymer supports and then aligned through the stretching of the polymer films[11, 53, 66]. This alignment results in polarizing films which absorb different wavelengths of light in the visible region simply by rotating the film. An additional use for metallic nanoparticles in the field

of photonics is in the development of waveguides which can transmit electromagnetic energy down a linear assembly of nanoparticles[31, 32].

1.3 Thesis Description

This thesis aims to establish techniques and principles that can be utilized to control the self-assembly of novel Nanomaterials into nanostructures. As the discussion in previous sections has shown, metallic nanoparticles are unique materials which can be used for optical, catalytic, electronic and sensing applications. Due to the vast number of techniques available to control the surface chemistry of these particles, there is a great deal of interest in utilizing metallic nanoparticles as building blocks in 'bottom-up' approaches to construct more intricate nanostuctures. By using self-assembly techniques, one can exploit natural chemical interactions to build complex constructs on the nanometer scale. Towards the goal of directed assembly of gold nanorods, synthesis and modification of nanorods with various polymers, inorganic oxides and organic ligands has been pursued. This thesis focuses on approaches for both irreversible and reversible self-assembly of gold nanorods in an end-to-end fashion.

The chapters which follow provide a detailed description of the research performed in this Masters Thesis project. Chapter Two discusses the seedless one-step synthesis of gold nanorods, which was the major procedure employed in this research, and the efforts to stabilize the gold nanorods in organic solvents through the deposition of polyelectrolyte layers. Chapter Three explores the

irreversible end-to-end assembly of gold nanorods utilizing a variety of simple organic ligands as well as the functionalization of the nanoparticles with silica for applications in nanoelectronics and MEMS (micro electro-mechanical systems) assembly. Chapter Four examines the novel reversible assembly of gold nanorods into linear chains through the use of a pH responsive polypeptide. Chapter Five summarizes the research presented in this thesis and concludes with a discussion on the direction for future work.

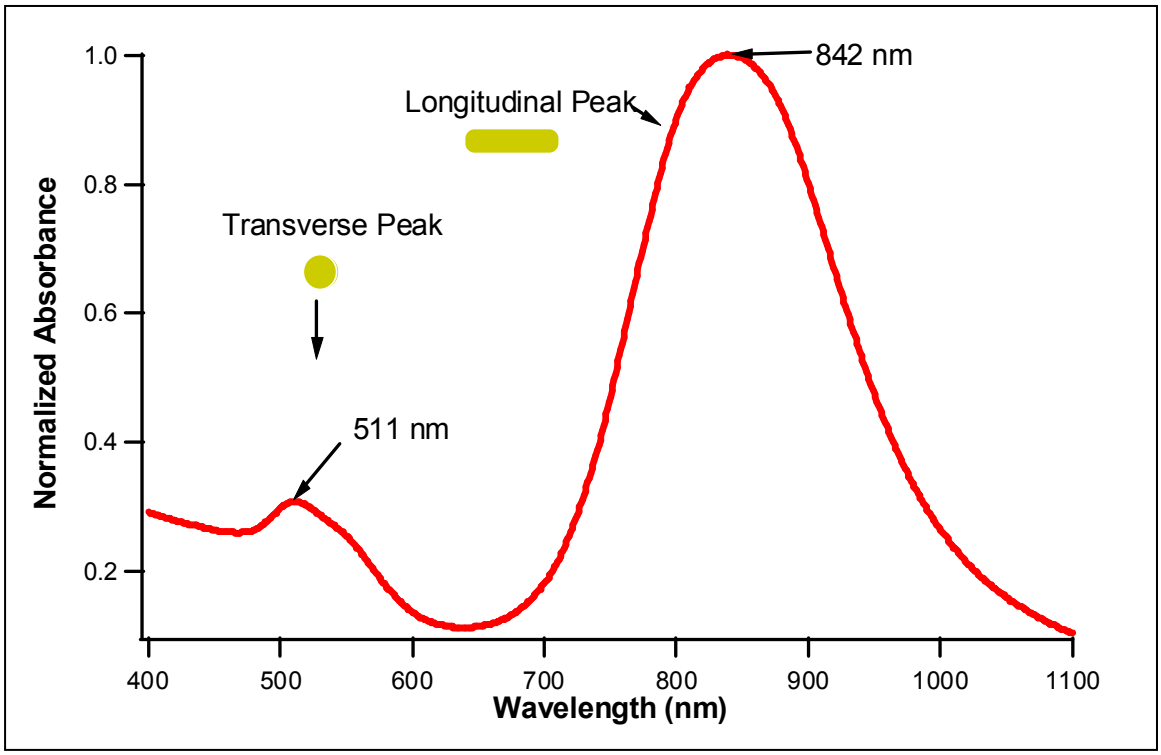

Figure 1.1: Optical Absorption Spectrum of Gold Nanorods

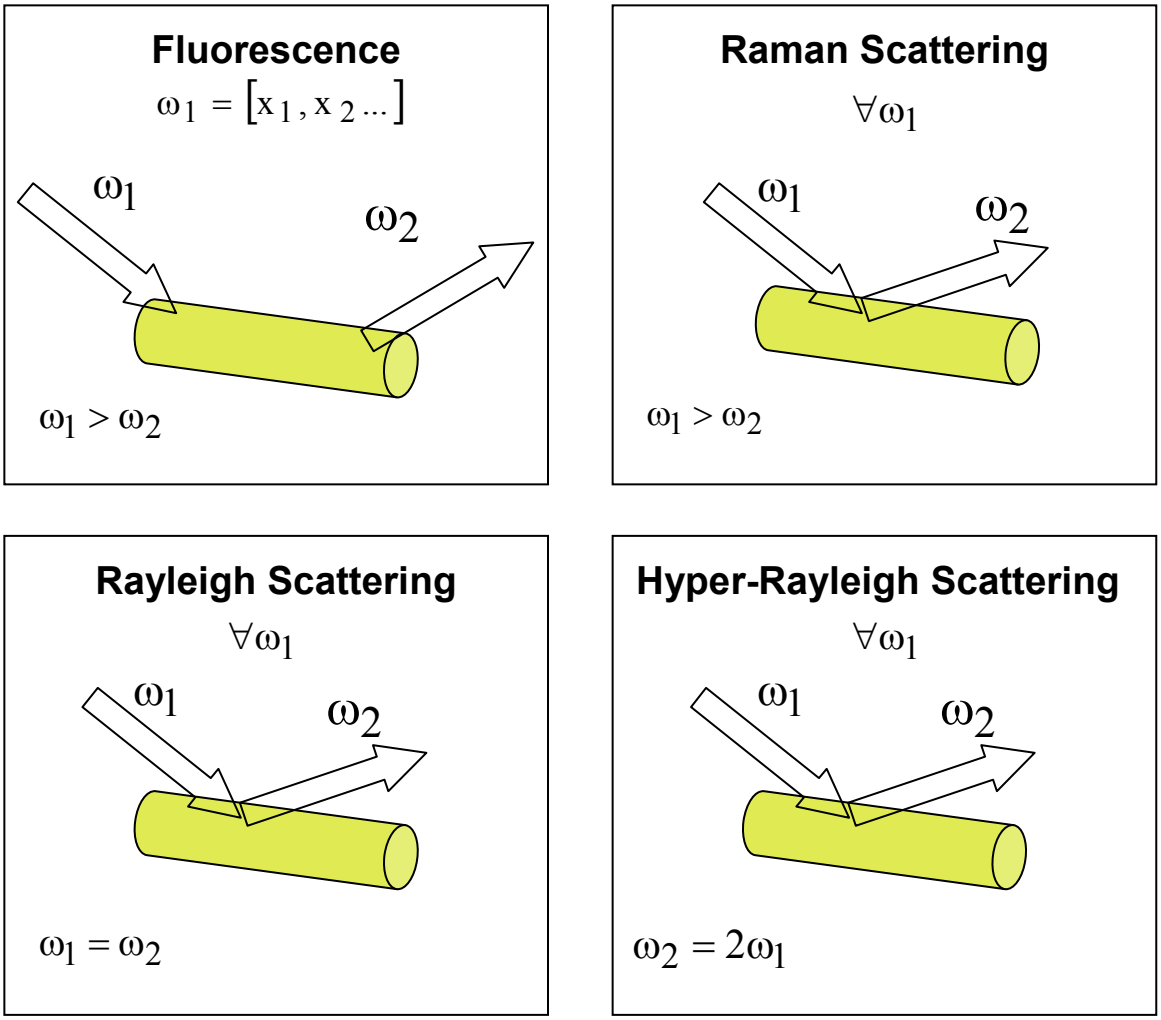

Figure 1.2: Optical Properties of Gold Nanorods

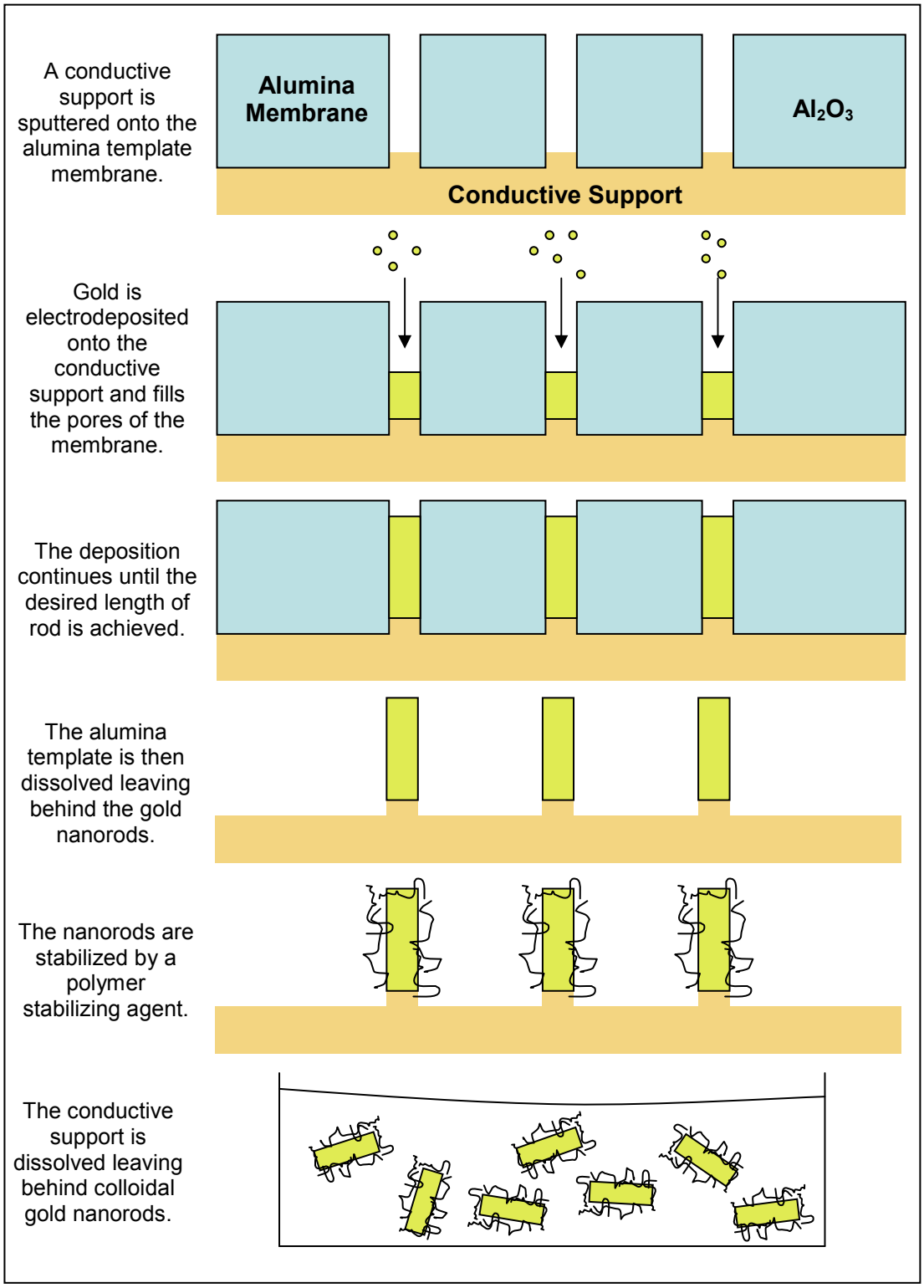

Figure 1.3: Schematic of Templated[42] Synthesis of Gold Nanorods

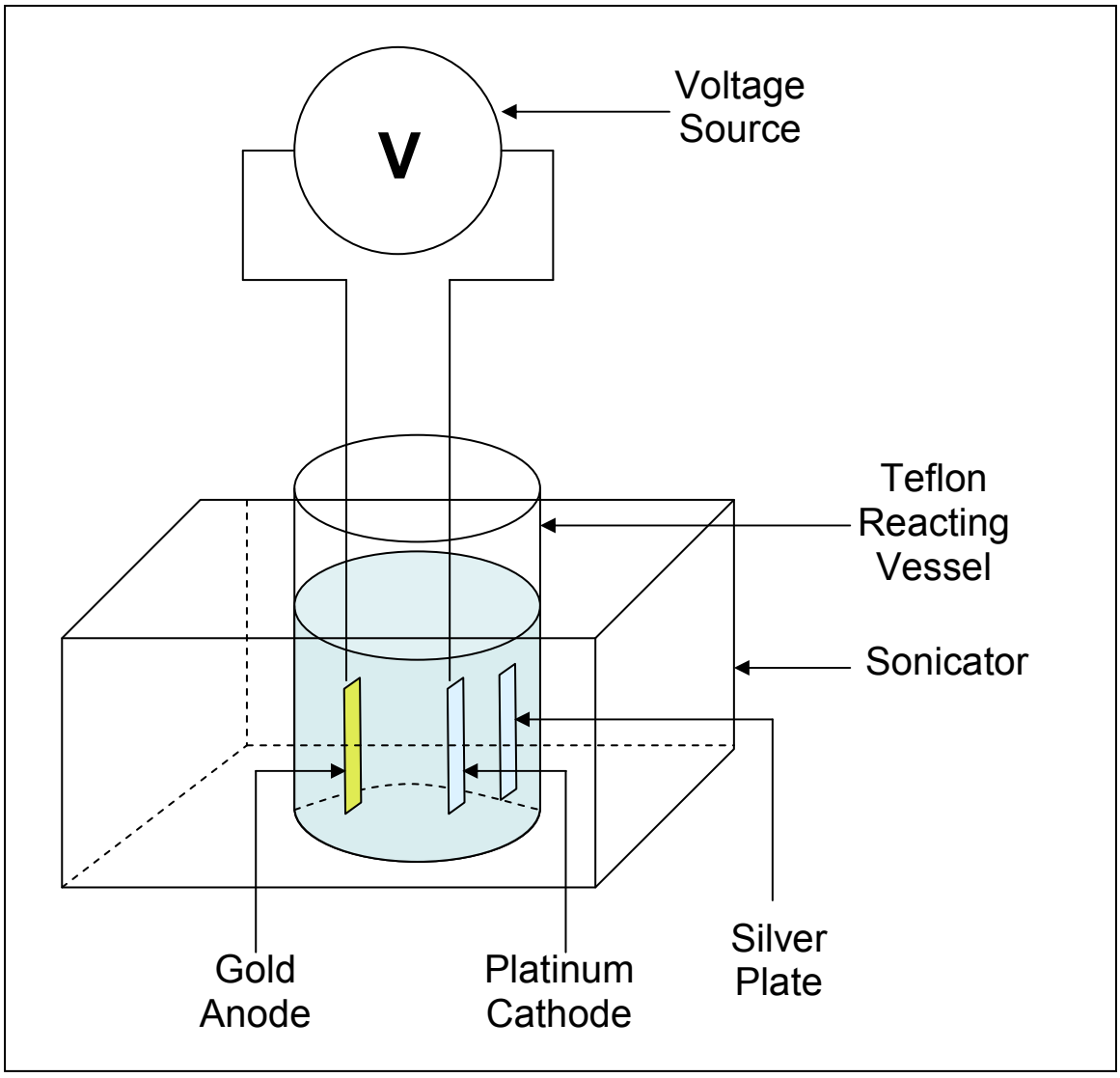

Figure 1.4: Schematic of Apparatus for Electrochemical[45] Growth of Gold Nanorods

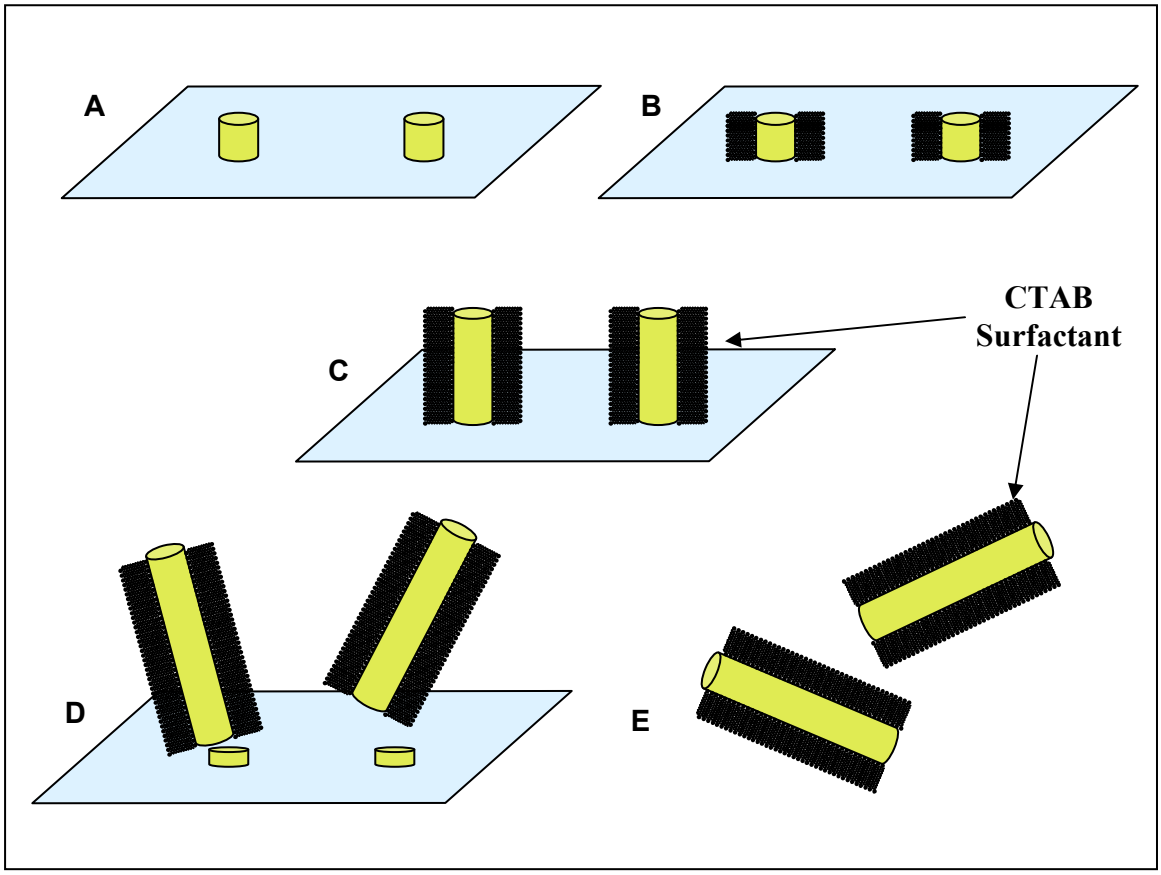

Figure 1.5: Schematic of Electrochemically[45] Deposited Gold Nanorods and Release by Sonication

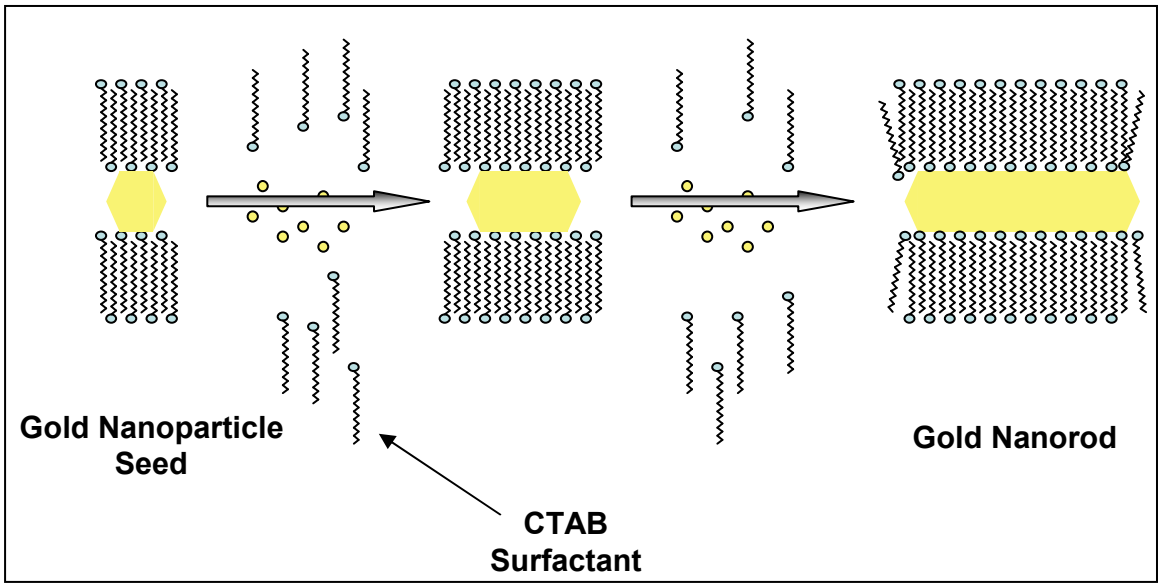

Figure 1.6: Schematic of Proposed 'Zipper' Mechanism[17]

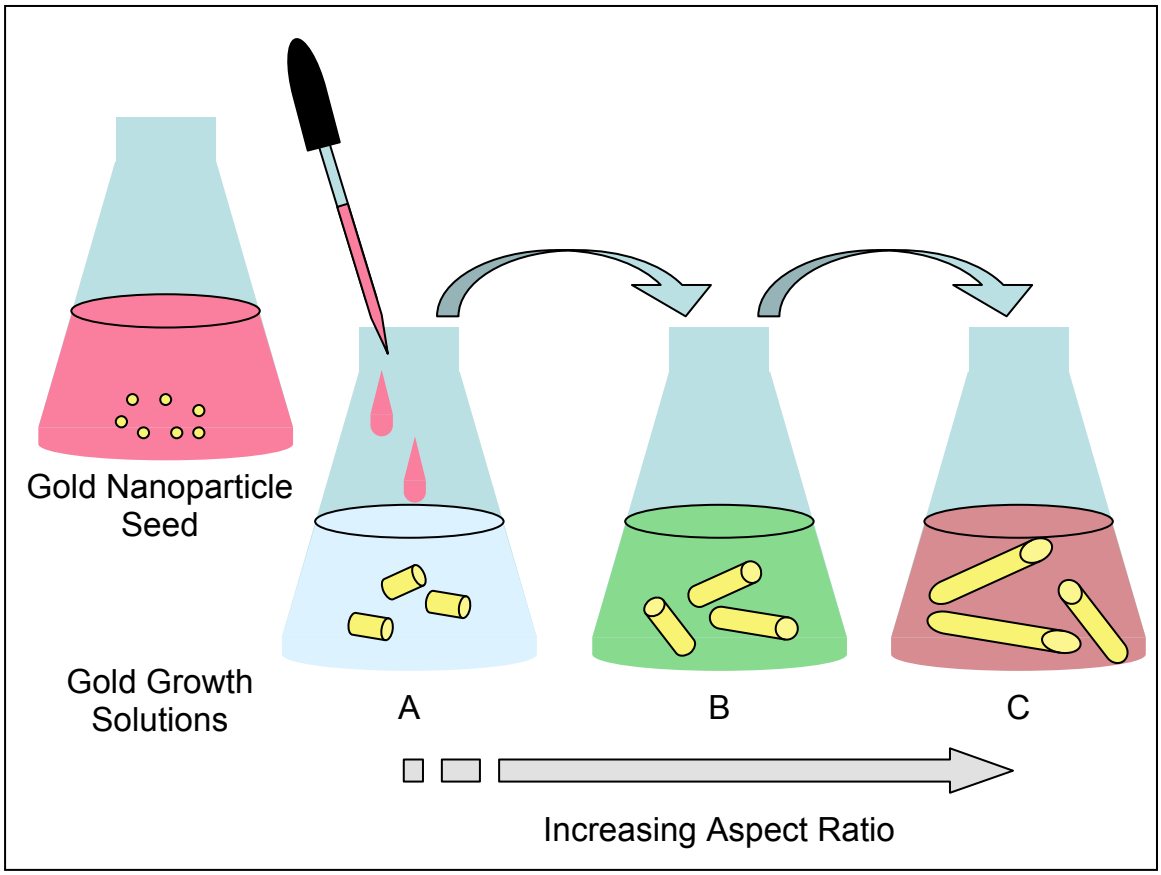

Figure 1.7: Seed Mediated Growth of Gold Nanorods Using Multiple Growth Solutions[17]

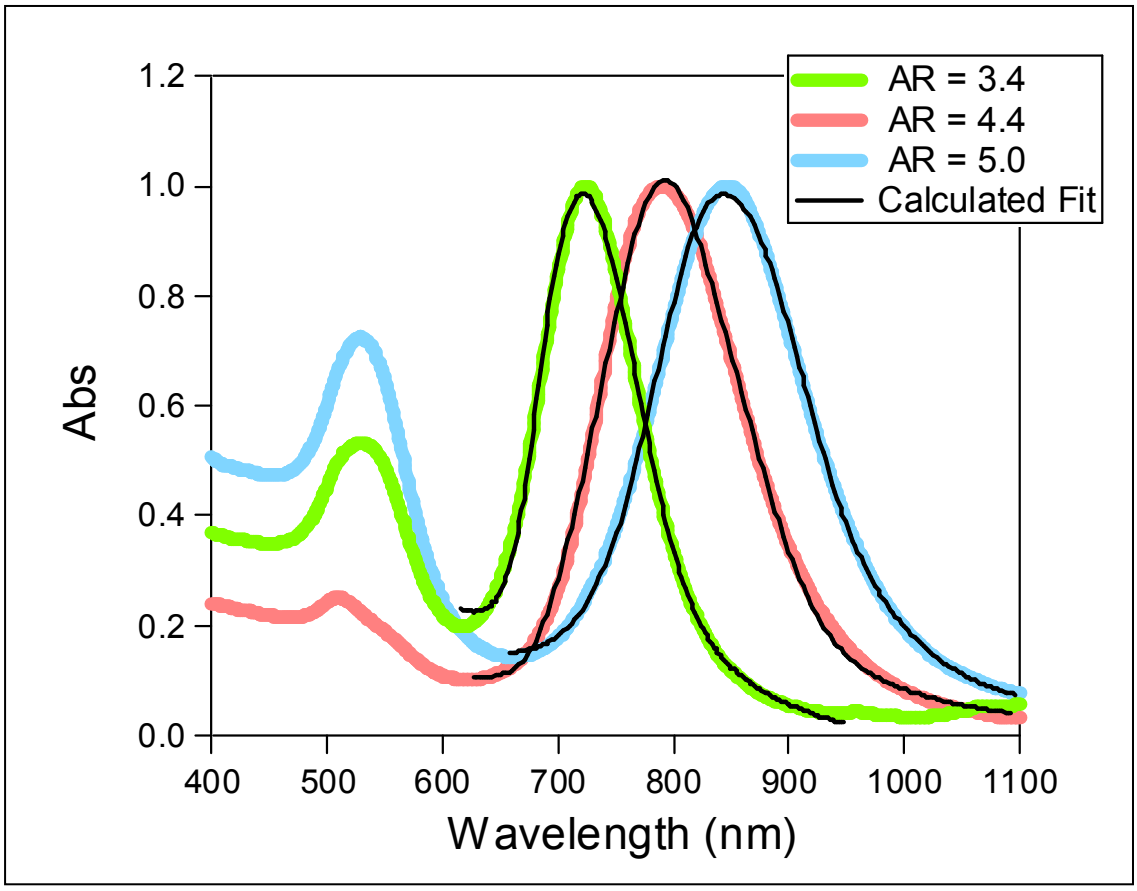

Figure 1.8: Experimental and Calculated Spectra of Gold Nanorods of Various Aspect Ratios

CHAPTER TWO: SYNTHESIS, CHARACTERIZATION, AND STABILIZATION OF GOLD NANORODS

2.1 Seedless Synthesis of Gold Nanorods

In this thesis, gold nanorods were prepared using a seedless synthesis of gold nanorods that is a simpler one-step procedure and is a modified version of the seed mediated method[19, 20, 24, 37]. As discussed in Chapter One, seed mediated methods require two steps: first, gold nanoparticles are synthesized and second, these particles are used as seeds in subsequent growth solutions to form gold nanorods. The seedless one-step synthesis procedure differs from the seed mediated procedure mainly in the fact that the gold nanoparticle seed is formed directly in a growth solution by the addition of a strong reducing agent to the growth solution[19, 24]. The seeds then continue to grow in the growth solution until the reactants become a limiting factor. It is believed that the reaction mechanism is identical to that of the seed mediated method. While no definitive proof exists, a proposed mechanism, often referred to as the 'zipper' mechanism[17], involves the directing surfactant assembly onto the particle simultaneously with the growth of the particle. The CTAB surfactant begins to adhere and form a bi-layer upon the {110} and {100} crystalline facets of the nanoparticles[50]. Growth of the particle along {110} and {100} crystalline facets is

hindered and directed growth of the particle occurs along the [001] axis with {111} facets as shown in Figure 2.1. This anisotropic growth eventually results in a cylindrically shaped particle where the {110} and {100} facets, which are protected by CTAB, are the sides of the nanorod with {111} facets near the ends[57, 60-63, 72]. As described in Chapter One, by controlling the reaction conditions during the synthesis procedure the aspect ratio of the particle can be tuned to a desired length[20, 21, 24].

2.1.1 Experimental

- Materials: $HAuCl_4$ (99.999%) was purchased from Sigma Aldrich. Silver nitrate ($AgNO_3$) was purchased through MP Biomedicals Inc. and L-ascorbic acid (99.2%) was purchased through Fisher Scientific. Cetyltrimethylammonium bromide (CTAB) (99+%) and sodium borohydride ($NaBH_4$ 98+%) powder were purchased through Acros Organics. Water used for all synthesis was purified using an EasyPure™ UV system (Barnstead, IA). A 0.2 μm filter incorporated into this system was used to remove any particulate matter.

- Seedless Synthesis of Gold Nanorods: Using a procedure adapted from Jana[19, 24], 30mL of 0.1 M aqueous CTAB solution was mixed with $HAuCl_4$, $AgNO_3$, and ascorbic acid such that the final concentrations were 4.4×10^{-4} M gold, 1.2×10^{-4} M $AgNO_3$, and 6.2×10^{-4} M ascorbic acid. The gold salt was reduced to form seed particles through the addition of 1mM $NaBH_4$

and the reaction mixture was allowed to rest undisturbed at a constant controlled temperature to ensure proper growth of gold nanorods. The gold nanorods were then purified through repeated centrifugations at 8500 rpm (~10,000g). The solids from each centrifugation were re-dispersed in de-ionized water to reduce the CTAB concentration. Typically two purification cycles were performed on each sample of gold nanorods resulting in a final concentration of approximately 10^{11} gold nanorods per mL as estimated by molar absorptivity[22] (~$5x10^{9}$ $M^{-1}cm^{-1}$). The purification procedure is portrayed in Figure 2.2.

- Characterization: UV-Vis spectra were recorded using a V-530 spectrophotometer (Jasco Inc., MD). TEM measurements were performed on a FEI Morgagni 268D operated at an accelerating voltage of 60 kV. Samples for TEM analysis were prepared by placing drops of colloidal solution on Formvar carbon coated copper grids (Electron Microscopy Sciences, PA). The colloidal solution was allowed to stand on the grid for 1 minute following which the extra solution was removed using a Kimwipe as blotting paper. The solvent was drawn from the side of the grid to prevent disruption of the sample leaving a thin layer of solvent to evaporate.

2.1.2 Results and Discussion

Figure 2.3 shows the UV-Vis spectrum of a typical gold nanorod sample which is stabilized with CTAB surfactant in water. The peaks located at 512 nm and 734 nm correspond to the transverse and longitudinal resonances of the gold nanorods, respectively. A TEM image of a typical gold nanorod sample is shown in Figure 2.4. From TEM images, gold nanorods produced by this method are typically 35 to 50 nm in length with aspect ratios ranging from approximately 3 to 4.5.

As discussed in Chapter One, the reaction conditions during the synthesis of gold nanorods can be controlled in such a way as to tune length of the gold nanorod[20, 21, 24]. The aspect ratio of the rod is directly related to the longitudinal resonance in the absorbance spectrum and, as shown in Figure 1.8, gold nanorods of various aspect ratios can be synthesized using this seedless one-step approach. The ability to tune the optical properties of these particles by controlling their length allows for a wide variety of applications[10, 21, 40, 58].

2.2 Layer-By-Layer Polyelectrolyte Coatings for Stabilization and Dispersion in Organic Solvents

In many applications it is necessary to stabilize and protect the CTAB bi-layer, which is responsible for the proper dispersion of the gold nanorods in solution as it is extremely sensitive to organic solvents and other electrostatic interactions. While several techniques exist for stabilizing nanoparticles, such as the use of inorganic oxide coatings[73-75] or changing the surface chemistry of the

particle through surface functionalization[6, 55], a common technique often employed is the electrostatic deposition of polyelectrolyte layers[9, 18, 52]. In some cases a single layer of polymer is all that is necessary to retain adequate dispersion while in other cases multiple layers of polyelectrolytes are required to effectively screen surface charges which can drive undesirable aggregation of particles.

2.2.1 Experimental

- Materials: Gold nanorods in an aqueous solution stabilized by CTAB surfactant are used in layer-by-layer depositions. Polyelectrolytes used include poly(vinyl pyrrolidone) (PVP) (10,000 MW), poly(acrylic acid) sodium salt (PAA) (35% wt. solution in water, 15,000 MW), and poly(allylamine hydrochloride) (PAH) (15,000 MW) from Sigma Aldrich. NaCl (ACS grade, certified) was secured from Fisher Scientific. Ethanol (200 proof) was purchased through Acros Organics. Water used for all synthesis was purified using an EasyPure^{TM} UV system (Barnstead, IA). A 0.2 μm filter incorporated into this system was used to remove any particulate matter.

- Layer-By-Layer Stabilization of Gold Nanorods: Initial attempts at re-dispersion of gold nanorods into ethanol were performed using the deposition of multiple polyelectrolyte layers through the layer-by-layer technique. Later, this technique was replaced by PVP stabilization due to

undesirable aggregation of gold nanorods during the layer-by-layer procedure. Aqueous stock solutions of polyelectrolytes with either a positive change, PAH, or a negative charge, PAA, were prepared to a concentration of 10 mg/mL and an aqueous stock solution of 20mM NaCl. In a typical coating procedure, before any polymers were deposited, 2mL of gold nanorods were centrifuged for 30 minutes at 8500 rpm (~10,000g) and re-dispersed to a volume of 2mL with 20mM NaCl. Approximately 400µL of PAA stock solution was added under vortex mixing and after the mixture was allowed to rest for a period of 5 minutes, it was centrifuged for 30 minutes and the supernatant was discarded to remove excess polymer. The solid residue of gold nanorods coated with CTAB and a layer of PAA were re-dispersed in 2mL of DI water containing 20mM NaCl. The polymer deposition was repeated using 400µL of PAH, a positively charged polyelectrolyte. Typically a total of four alternating layers of PAA and PAH were deposited (2 each) using this technique.

- PVP Stabilization of Gold Nanorods: To re-disperse the gold nanorods in ethanol, the nanorods were stabilized with PVP using a procedure, that was adapted from Liz-Marzán and co-workers[52, 76]. In a typical procedure, 10mL of aqueous gold nanorods stabilized by CTAB were mixed with 2.5mL of a 10mg/mL PVP aqueous stock solution under vigorous vortex mixing. The addition was performed slowly in 4 equivalent aliquots spaced five to ten minutes apart. The solution was then allowed to mix

under gentle vortex action for a minimum of 24 hours, which allowed adequate time for the PVP to assemble onto the gold nanorods. The sample was subsequently centrifuged at 8500 rpm (~10,000g) for 30 minutes and the supernatant discarded to remove excess PVP. The gold nanorod residue was then re-dispersed in pure ethanol and other polar organic solvents such as DMF or chloroform, which would typically cause the immediate aggregation of CTAB stabilized gold nanorods when no polymer layers are present.

- Characterization: UV-Vis spectra were recorded using a V-530 spectrophotometer (Jasco Inc., MD). TEM measurements were performed on a FEI Morgagni 268D operated at an accelerating voltage of 60 kV. Samples for TEM analysis were prepared by placing drops of colloidal solution on Formvar carbon coated copper grids (Electron Microscopy Sciences, PA). The colloidal solution was allowed to stand on the grid for 1 minute following which the extra solution was removed using a Kimwipe as blotting paper. The solvent was drawn from the side of the grid to prevent disruption of the sample leaving a thin layer of solvent to evaporate.

2.2.2 Results and Discussion

Past studies have shown that the stabilizing surfactant bi-layer of CTAB maintains a positive zeta potential which can be used to drive the electrostatic

assembly of stabilizing polymer layers onto the surface of the nanorod[52, 76]. These polymer layers stabilize the gold nanorods through electrostatic repulsive forces that are strong enough to maintain dispersion while simultaneously screening the strong surface charge of the CTAB surfactant.

The stabilization of gold nanorods using polymer layers is required in this research for two reasons: first, many molecules which can be used to functionalize gold nanorods are not soluble in aqueous environments and it is necessary to disperse the gold nanorods in organic solvents where the stabilizing CTAB bi-layer is unstable. Secondly, some molecules used to functionalize the gold nanorods have strong electrostatic interactions with the CTAB bi-layer and induce the aggregation of particles upon their addition. Polymeric stabilization offers a solution to both of these problems.

Figure 2.5 outlines two pathways towards the stabilization of gold nanorods utilizing the deposition of polymer layers. In the first method, multiple layers of polyelectrolytes of alternating charges are deposited onto the surface of the nanorod to protect the CTAB bi-layer from outside electrostatic interactions. In the second approach a single layer of PVP is deposited to partially screen the charge of the CTAB surfactant. In this approach the electrostatic interactions between the CTAB bi-layer and exterior influences are minimized by weakening the strong surface charge of the particle. The slightly negative polyelectrolyte reduces the surface charge of the CTAB bi-layer from a strong positive charge to a weak positive charge[52, 76].

Figure 2.6 shows the optical spectra of gold nanorods stabilized with PVP that are successfully re-dispersed in multiple organic solvents. The process of multi-layer stabilization of gold nanorods was abandoned due to the aggregation of particles during the coating procedure, as seen in Figure 2.7. The single layer of PVP provides sufficient stability to disperse the gold nanorods in organic solvents while maintaining unaggregated gold nanorods as seen in Figure 2.8. Due to the increase in the refractive index from water to ethanol (n=1.33 to n=1.36), or other organic solvents, a red-shift is observed in both the transverse and longitudinal peaks of the PVP stabilized gold nanorods. This red-shift is expected and has been observed in previous experimentation and calculations[18, 36, 52, 76].

While it has been shown that the addition of polyelectrolyte layers causes the transverse resonance to shift to higher wavelengths[18, 36, 52, 76], no appreciable shift is observed following the PVP coating. It is assumed that the lack of this red-shift following the deposition of PVP indicates that the layer of polymer deposited is extremely thin. This belief is supported by the TEM imaging where no polymer layer can be observed surrounding the gold nanorods, which is contrasted to the scenario of the multi-layer polymer coated gold nanorods where polymer coatings are observed by TEM images. While the contribution of the PVP layer is not discernible in the absorption spectrum or TEM images, the stable re-dispersion of the PVP coated gold nanorods into ethanol is achieved leading to the conclusion that gold nanorods were successfully coated with PVP.

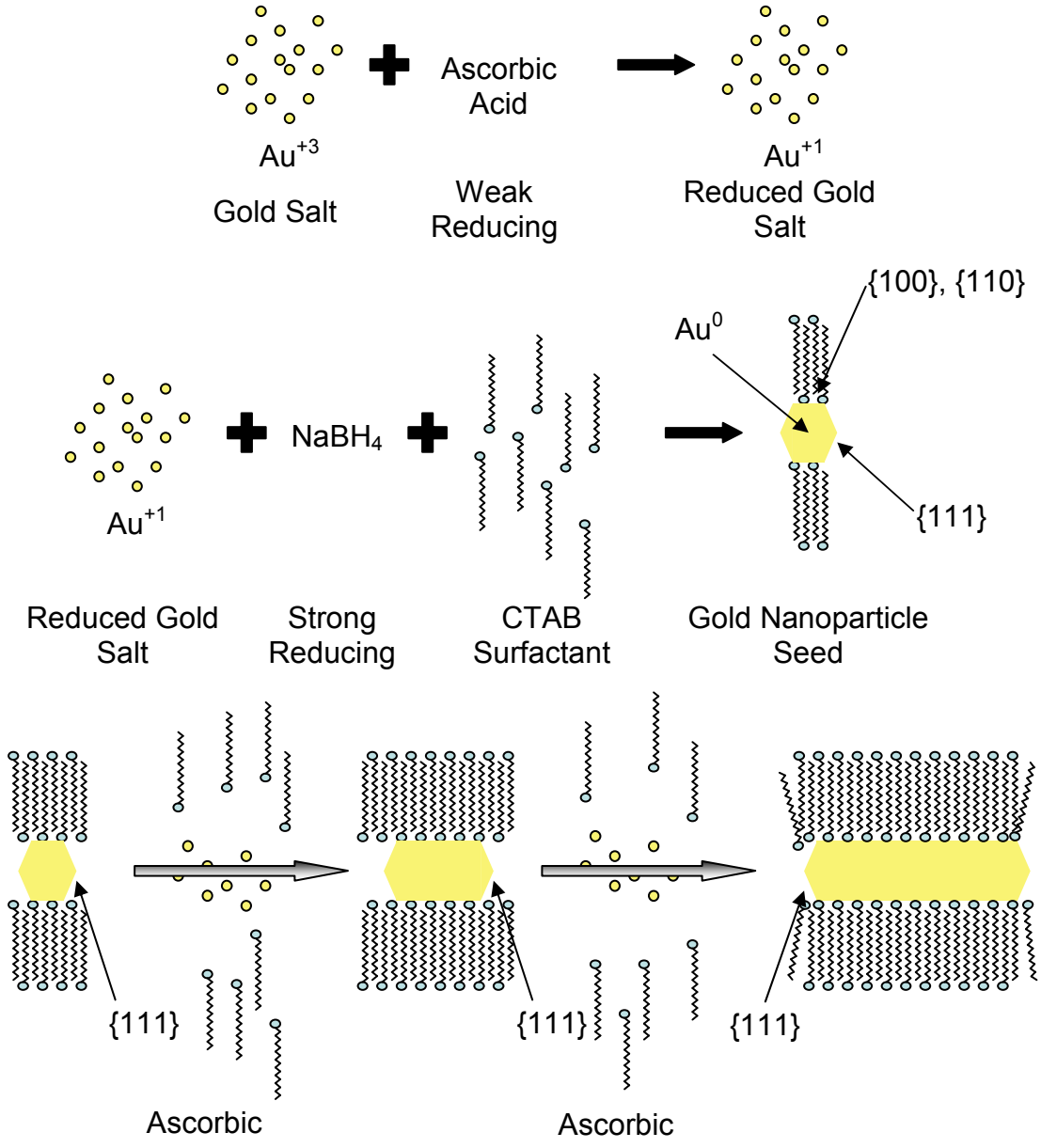

The presence of ascorbic acid, a weak reducing agent, allows Au^{+1} to reduce to Au^{+0} on the surface of the gold seed. In this manner, the ascorbic acid facilitates the growth of the nanorod without allowing the formation of any new seeds. The CTAB surfactant hinders growth of specific crystalline facets resulting in an anisotropic growth and the formation of the gold nanorod.

Figure 2.1: Schematic of Growth of Gold Nanorods in Solution

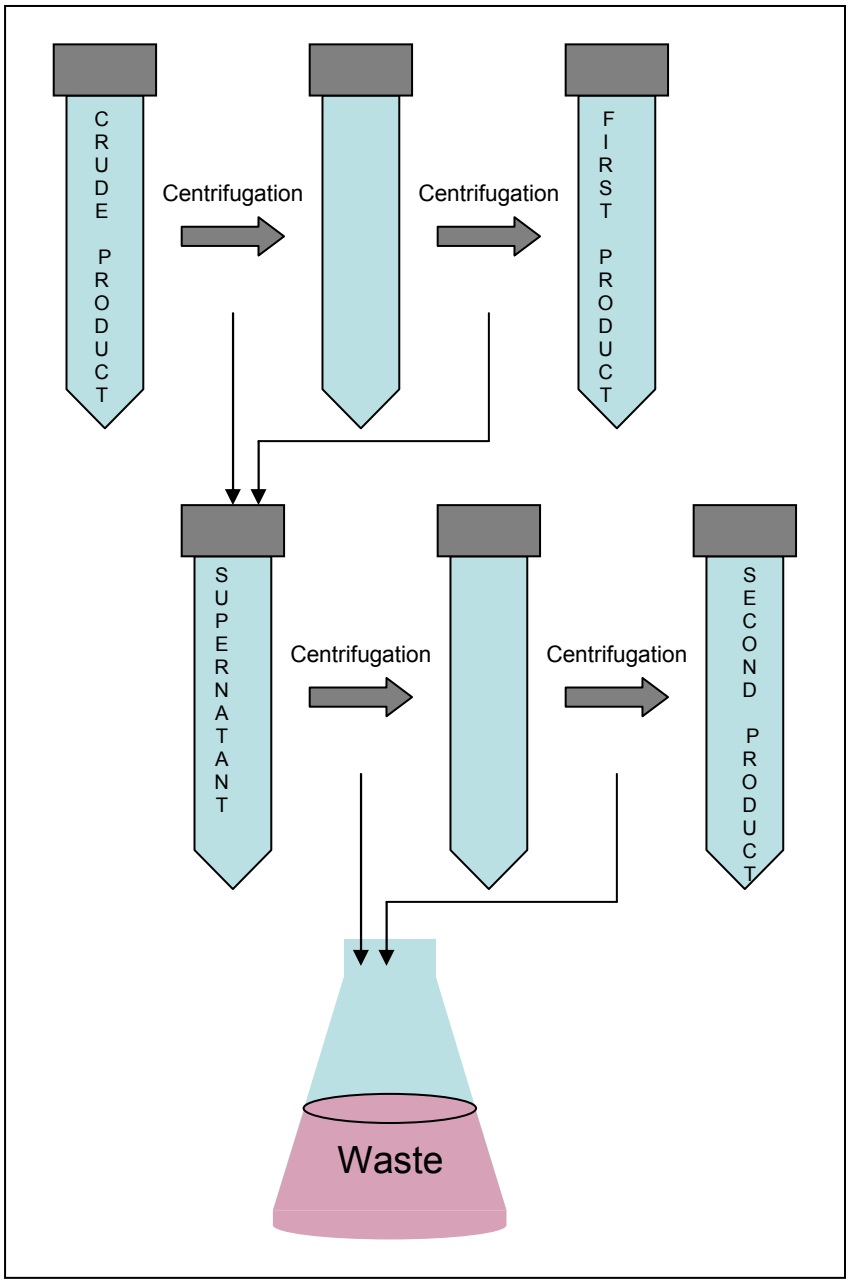

Figure 2.2: Schematic of Purification Procedure of Gold Nanorods

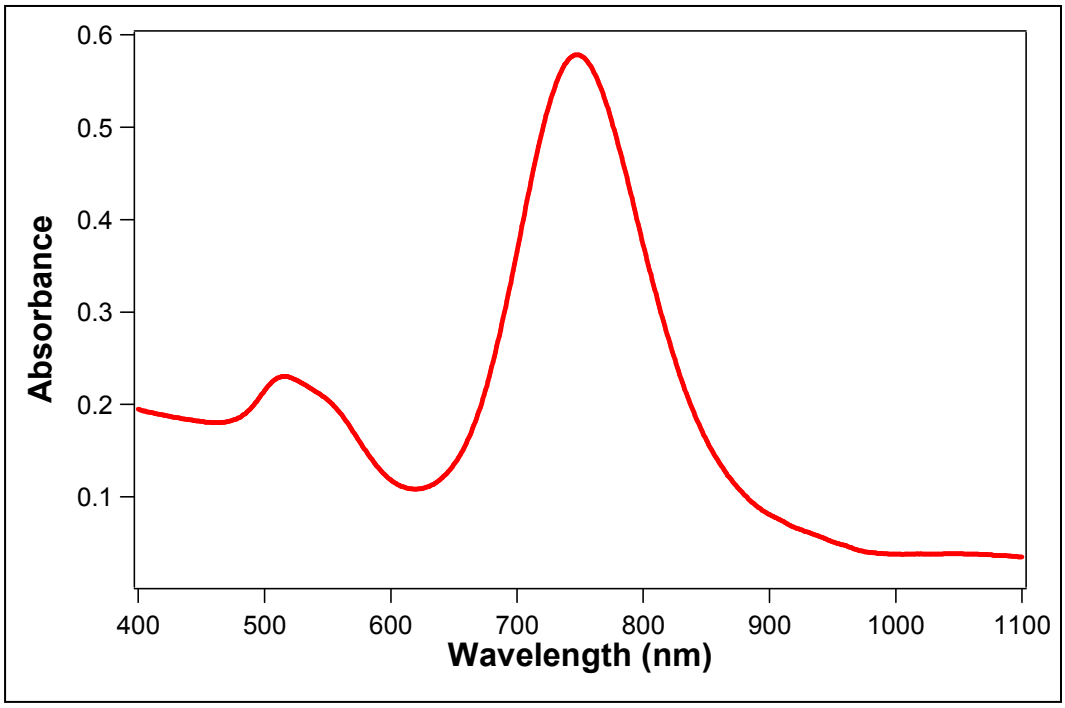

Figure 2.3: Optical Spectrum of Gold Nanorods

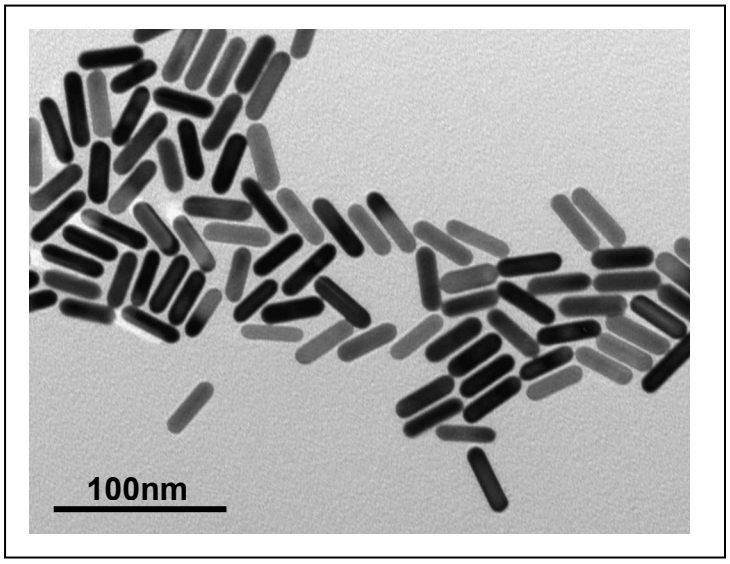

Figure 2.4: TEM Image of Gold Nanorods

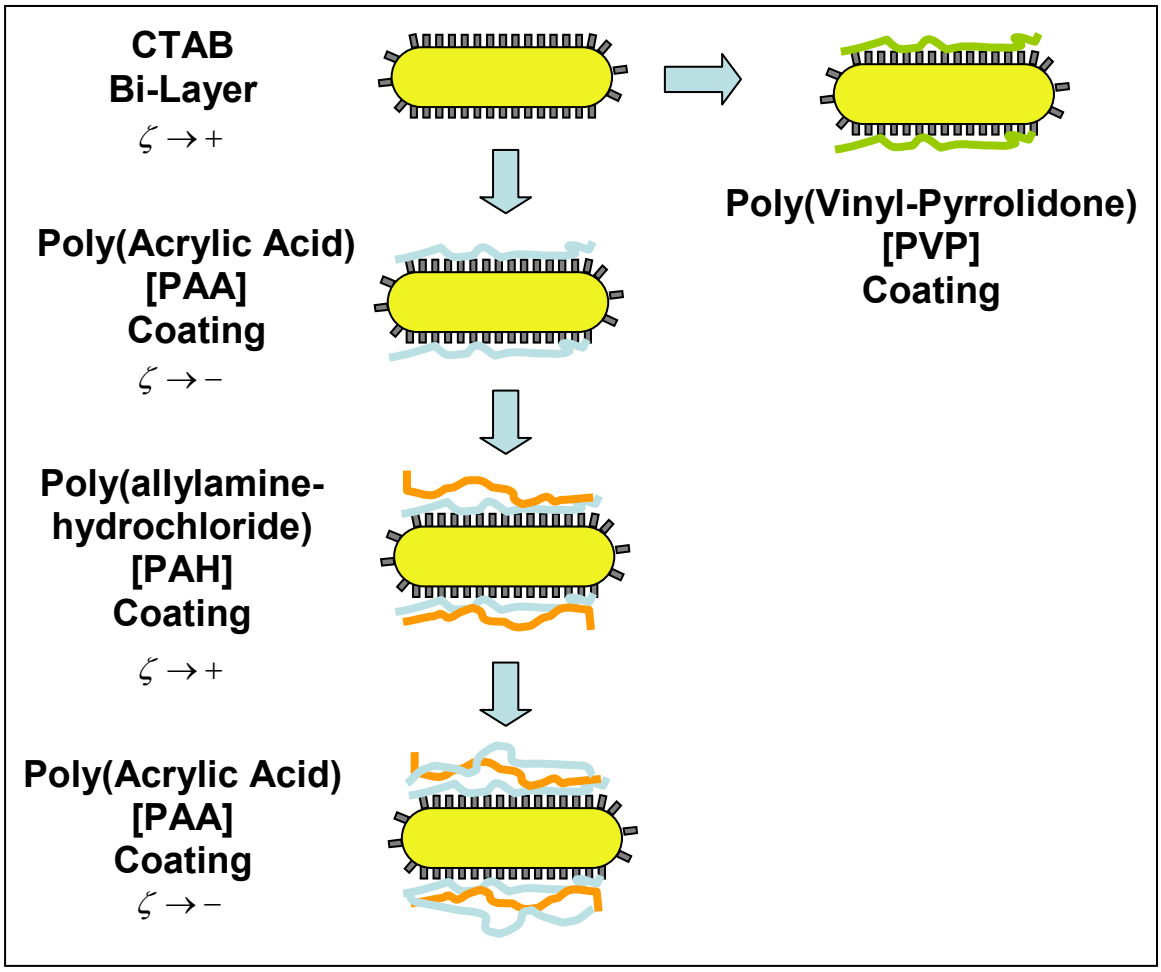

Figure 2.5: Schematic of Layer-by-Layer Coating of Gold Nanorods

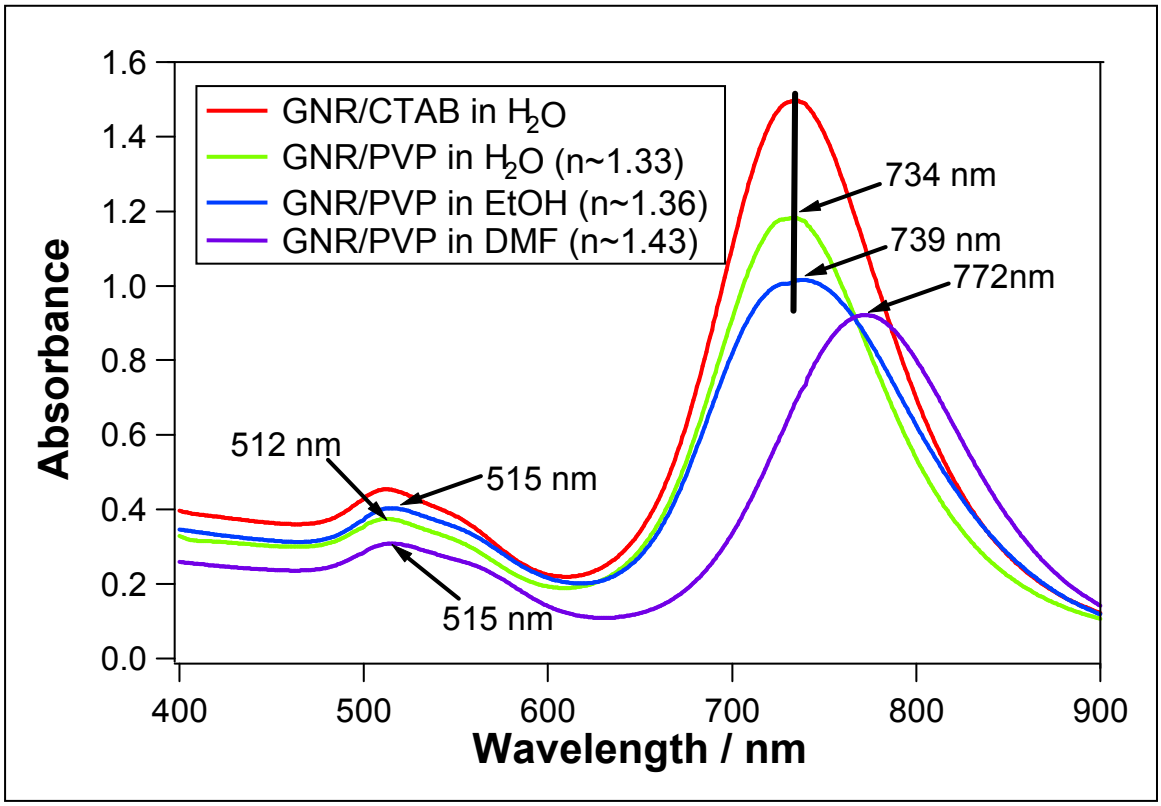

Figure 2.6: Optical Spectra of Polymer Stabilized Gold Nanorods in Organic Solvents

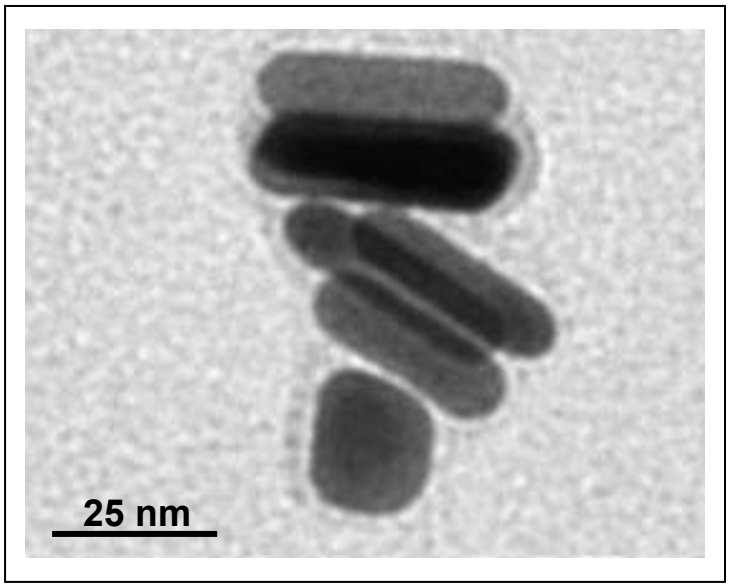

Figure 2.7: TEM Image of PAA and PAH Coated Gold Nanorods

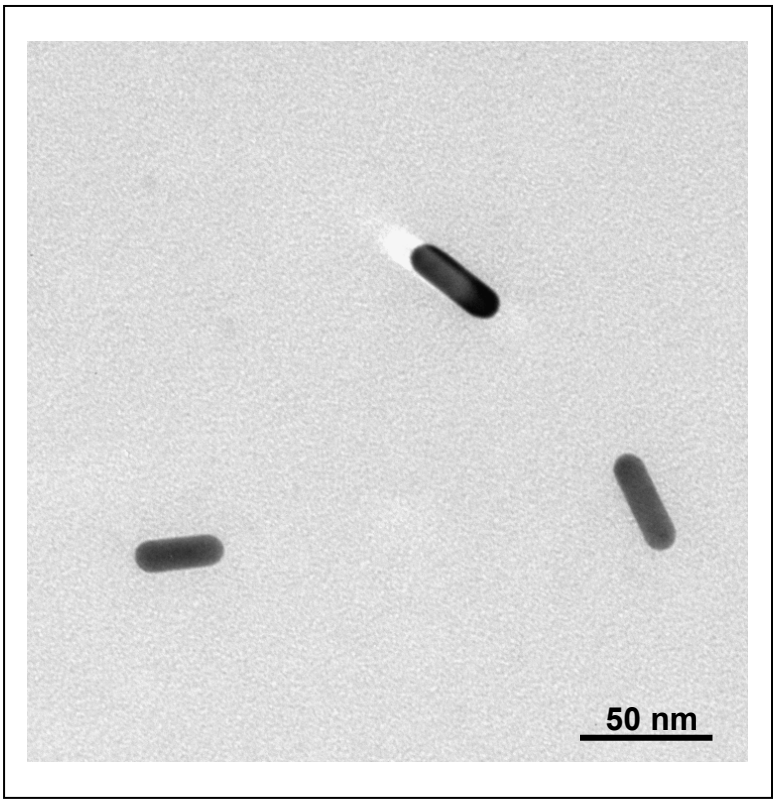

Figure 2.8: TEM Image of PVP Stabilized Gold Nanorods

CHAPTER THREE: IRREVERSIBLE ASSEMBLY OF GOLD NANORODS

3.1 Assembly of Gold Nanorods Using Bifunctional Organic Ligands

The directed self-assembly of gold nanorods into one-dimensional nanostructures through end-to-end linking has been attempted in the recent past utilizing an array of techniques. While the molecular interactions driving the assembly process might vary, in these approaches, almost universally, the ends of the gold nanorods are selectively functionalized with organosulfides containing either a thiol or a disulfide functional group. Following this end-functionalization, various chemical or hydrogen bonding interactions between the molecules are then exploited to drive the assembly process[21, 58-61, 63]. Examples of these irreversible techniques include the end-to-end assembly of gold nanorods using hydrogen bonding between organic ligands with terminal carboxylic and/or amino groups[29, 59, 61, 63], streptavidin mediated linkage using disulfide modified biotin molecules[57], short dithiol molecules[60], as well as disulfide modified antibody-antigen interactions[58].

In all of the above investigations, the assembly of gold nanorods often produced linear chains of varying lengths or branched complexes. None of these assembly techniques have been shown to be reversible in nature. Mann and co-workers pursued the reversible assembly of gold nanorods through the use of

complimentary strands of thiolated DNA which could be thermally decomposed to reverse the process[77]. For reasons yet to be explained, the assembly of nanorods using this technique was found to be irreversible. Polymer functionalized gold nanorods have been assembled into ring structures by using water droplets as templates[8] or significant changes in solvent-polymer interactions[78]. The latter has been shown to be reversible upon the addition of a large fraction good and bad of solvents for the polymer chains.

This section examines the irreversible assembly of gold nanorods stabilized in ethanol using a handful of the afore-mentioned techniques. First, cysteine and glutathione was utilized to drive the assembly through hydrogen bonding between the carboxylic acid or amino functional groups. 1,6-Hexanedithiol was then used to assemble the gold nanorods through stronger chemisorption of the thiol. These initial irreversible assemblies are important because they can be used to confirm that the end functionalization of the PVP modified gold nanorods is still possible as well as to provide a basis for which to contrast to the reversible linking phenomena discussed in Chapter Four of this work.

While all three of these simple organic molecules have been used before to drive self-assembly, our study has several unique differences which depart from previous research. The synthesis of all gold nanorods which were utilized in this work was performed using through the one-step seedless method. This methodology of preparing gold nanorods was not used by any of the groups that have previously reported end-to-end assembly. This is significant because it

would indicate that regardless of the preparation technique, functional groups containing sulfur will preferentially bind to the ends of the gold nanorods prepared by the seedless one-step method. This work is also divergent from other works in the respect that the gold nanorods were first stabilized with PVP and the organic solvent used in this process being ethanol. In other works, a solvent mixture of acetonitrile and water was often reported[59-61]. In an attempt to reproduce these works we found that our as-prepared gold nanorods were not stable in this mixture directly and would have to be stabilized before being transferred into organic solvents. One other group, Stucky and co-workers, reported similar results in dispersion of gold nanorods into the acetonitrile and water mixture[63], and chose to pursue the assembly in strictly aqueous conditions. In our approach, we have functionalized and assembled the gold nanorods in an ethanol and water mixture. While the system is stable in pure ethanol a smaller amount of water must be present for assemblies where the zwitterionic molecules, such as cysteine and glutathione, are used to drive the assembly.

3.1.1 Experimental

- Materials: Ethanol (200 proof), L-Cysteine, (99+%), Glutahione (98%), and 1,6-hexanedithiol (97%) were purchase from Acros Organics. Water used for all synthesis was purified using an EasyPure^{TM} UV system (Barnstead, IA). A 0.2 μm filter incorporated into this system removed particulate matter.

- Assembly by Cysteine Functionalized Gold Nanorods: The irreversible assembly of gold nanorods with cysteine was performed in an ethanol and water mixture. Approximately 500μL of PVP stabilized gold nanorods were diluted with an addition 500μL of ethanol in a cuvette. The assembly of cysteine molecules on the ends of the gold nanorods was performed in pure ethanol through the addition of 20μL of 6.74mM cysteine in ethanol stock solution. After approximately 1 hour which allows sufficient time for the cysteine molecules to assemble into a monolayer on the ends of the gold nanorods, 200μL of water was added to the cuvette. The cuvette was then capped and mixed by three successive inversions. The assembly of the cysteine monolayer on the ends of the gold nanorods as well as the subsequent end-to-end assembly of the gold nanorods was monitored continuously by UV-Vis spectroscopy. The final pH of the system was also measured and determined to be 7.31.

- Assembly by Glutathione Functionalized Gold Nanorods: The irreversible assembly of gold nanorods with glutathione was performed in an ethanol and water mixture and was carried out identically to the assembly by cysteine functionalized gold nanorods. The only variation in the procedure was that rather than adding 20μL of a 6.74mM cysteine in ethanol stock solution, 40μL of a 3.47mM glutathione in ethanol stock is utilized. The remainder of the experiment and characterization was similar to the

cysteine assembly. The final pH of the system was also measured and determined to be 7.35.

- Assembly by 1,6-Hexanedithiol Functionalized Gold Nanorods: The irreversible assembly of gold nanorods with 1,6-hexanedithiol was performed in an ethanolic solution. 200µL of PVP stabilized gold nanorods were diluted with an addition 800µl of ethanol in a cuvette. To the cuvette, 10µL of a 6.28mM 1,6-hexanedithiol stock solution was added to a cuvette. The end-to-end assembly of the gold nanorods was monitored continuously by UV-Vis spectroscopy and DLS. TEM grids were prepared at various points throughout the assembly process for further characterization at a later time.

- Characterization: UV-Vis spectra were recorded using a V-530 spectrophotometer (Jasco Inc., MD). Dynamic light scattering (DLS) measurements were performed at 20^{o}C using a Zetasizer Nano-S (Malvern Instruments, PA) which was equipped with a red laser (633 nm) and a detector for analyzing backscattering at 173^{o} from the incident light. All pH measurements were performed using an Accumet electrode from Fisher Scientific (Catalog Number 13-620-290) attached to a Cole-Palmer pH/mV/^{o}C bench top meter (Model Number 59003). TEM measurements were performed on a FEI Morgagni 268D operated at an accelerating voltage of 60 kV. Samples for TEM analysis were prepared by placing

drops of colloidal solution on Formvar carbon coated copper grids (Electron Microscopy Sciences, PA). The colloidal solution was allowed to stand on the grid for 1 minute following which the extra solution was removed using a Kimwipe as blotting paper. The solvent was drawn from the side of the grid to prevent disruption of the sample leaving a thin layer of solvent to evaporate.

3.1.2 Results and Discussion

The assembly of gold nanorods through the use of cysteine and glutathione has been previously reported by multiple research groups[59, 63]. In all of these cases, gold nanorods were never synthesized by the one-step seedless method, stabilized by a PVP, or dispersed in ethanol. The assembly of the gold nanorods in an end-to-end fashion is driven by hydrogen bonding between either the cysteine or glutathione molecules, which are functionalized onto the ends of the nanorods. A schematic of the proposed assembly is depicted in Figure 3.1.

The functionalization with either the cysteine or glutathione molecules was carried out in pure ethanol as it is a medium in which the PVP modified gold nanorods are stable and which cysteine and glutathione are readily soluble. Because this process is carried out in pure ethanol, the sample does not assemble into linear chains at this point because the assembly is driven by zwitterionic functional groups that require the presence of water. It has been shown by Stucky and co-workers that a pH of approximately 4 is optimal for the end-to-end assembly by these zwitterionic functional groups[63]. In Figure 3.2, the

UV-Vis spectrum of gold nanorods is shown before the addition of cysteine (curve a) and after the formation of the cysteine monolayer (curve b). It should be noted that a slight red-shift is observed in both the transverse and longitudinal resonances, which is indicative of a change in the refractive index surrounding the particle and the formation of a monolayer[16, 35, 36]. This slight red-shift is also seen in the assembly of the glutathione monolayer in Figure 3.3, where the transverse and longitudinal peaks are both red-shifted after the assembly of the monolayer (curve b). This red-shift is to be expected when functionalizing the particle with a dielectric coating as is the case here.

Following the functionalization of the gold nanorod, a small quantity of water (neutral pH) is added directly to the cuvette. It is only upon this addition that the end-to-end assembly of gold nanorods occurs as evident in multiple control experiments. The vast majority of this assembly process occurs within the first ten minutes for the cysteine and then continues more slowly for the remainder of an hour. In the case of glutathione, the assembly in an end-to-end fashion proceeds slower than the assembly by cysteine, but the majority of the assembly process occurs within the first hour. Figure 3.2 (curves c to k) and Figure 3.3 (curves c to l) depicts the assembly process driven by the cysteine modified gold nanorods and the glutathione modified gold nanorods respectively through the UV-Vis spectra that were collected as a function of time. The formation of an isobestic point at approximately 800 nm is indicative of linear assembly phenomena[57, 59, 60, 63, 77]. The isobestic points depicted in Figure 3.2 and Figure 3.3 indicates that two populations of gold nanorods must be changing

simultaneously. It is believed that the first population is composed of single gold nanorods, which have a longitudinal resonance at 752 nm, and the second population being the linked gold nanorods, which due to a uniaxially coupled longitudinal plasmon resonance has a peak absorption at higher wavelengths close to 900 nm. This second population will continue to red-shift continuously as the linear chains begin to grow longer and the coupled longitudinal resonance of the nanoparticles increases[61, 79].

The assembly of gold nanorods by dithol molecules of various lengths has also been previously investigated by Thomas and co-workers[60] and is depicted in Figure 3.4. As is the case of the cysteine and glutathione mediated assemblies, two important differences exist between this past study and the present results. First, Thomas and co-workers prepared the gold nanorods using a photochemical method as opposed to the one-step seedless method that we have utilized. Second, the surfactant stabilized gold nanorods used by Thomas and co-workers were dispersed directly in a mixture of acetonitrile and water which, as was discussed earlier, resulted in the immediate aggregation of our as prepared nanoparticles. For this reason, this research has utilized gold nanorods stabilized by PVP in ethanol.

The end-to-end assembly of gold nanorods using the dithiol was monitored using UV-Vis spectroscopy, DLS, and TEM analysis. The assembly of gold nanorods into linear chains after the addition of a small amount of hexanedithiol can be observed as a function of time in the UV spectra shown in Figure 3.5. As the gold nanorods assemble in a linear fashion an isobestic point

is formed similar to the assembly of gold nanorods using cysteine and glutathione. As the self-assembly continues, plasmon coupling occurs in the longitudinal resonance of the gold nanorods and results in the continued red-shift of this resonance[61, 79]. This can be observed in the spectra of the hexanedithiol assembly shown as a function of time in Figure 3.5.

TEM images were collected at various points in the assembly process to document information relating to the extent of linking and the longitudinal resonance of the gold nanorods. Figure 3.6 depicts the state of the gold nanorods before the assembly occurs (t=0 min) and at continually increasing times in the reaction (t=57 min, t=79 min).

DLS measurements were also recorded for this process to gather information relating to the size of the chains during the assembly process. It is known that the intensity autocorrelation function can be related to the translational diffusion coefficient of the particle, which depends on the size and aspect ratio of the nanorods[80, 81]. In Figure 3.7 the autocorrelation functions are plotted at advancing times during the assembly process and have been selected to correlate as closely to the images shown in Figure 3.6 as possible. It can be seen in this figure that the correlation function continues to shift to longer decay times as the self-assembly proceeds and a smaller effective diffusion coefficient for the assembled particles becomes dominant. A future goal is to use DLS with polarized light to prove changes in the aspect ratio of the nanorod complexes and to explore changes in both the rotational and translational diffusion coefficients[80, 81].

3.2 Assembly of Gold Nanorods Using Inorganic Oxides

The coupling of gold nanorods with inorganic oxides has been explored by past researchers[73-75, 82, 83], but no reports exist on this approach being exploited for directed assembly of nanorods into complex nanostructures. Towards this end, gold nanorods functionalized with an organic inorganic hybrid molecule, 3-Mercaptopropyl Trimethoxysilane (MPTMS), have been assembled the into end-to-end coupled complexes via condensation reaction. These complexes have also led to the question of whether one can control silica deposition on gold nanorods and selectively deposit it on the ends of the nanorods. Silica was deposited through the use of sodium metasilicate using two procedures which produced different results. In one method, the metasilicate is deposited slowly onto the MPTMS functionalized gold nanorods and results in gold nanorods coated in the thin even layer of SiO_2. The second procedure performed involved the rapid deposition of silica through a forced precipitation. This rapid reaction resulted in irregular coatings of silica which were preferentially around the ends of the gold nanorods. While this methodology requires further refinement, it offers a route for the development of gold nanorods which are end functionalized with SiO_2 and can provide an alternative approach to end-functionalizing gold nanorods by exploiting interactions of silane derivatives with silica.

3.2.1 Experimental

- Materials: Ethanol (200 proof) and 3-Mercaptopropyl Trimethoxysilane (85% Tech. Grade) were purchase from Acros Organics. Sodium

Metasilicate (44-47%) was purchased from Sigma Aldrich. Water used for all synthesis was purified using an EasyPure™ UV system (Barnstead, IA). A 0.2 μm filter incorporated into this system removed particulate matter.

- Assembly by Condensation of MPTMS Functionalized Gold Nanorods: The irreversible assembly of gold nanorods with MPTMS was performed in an ethanol and water mixture. 500μL of PVP stabilized gold nanorods were diluted with an addition 500μL of ethanol to a total volume of 1mL in a cuvette. The assembly of the MPTMS molecules onto the ends of the gold nanorods was performed in pure ethanol through the addition of 10μL of a 6.96mM MPTMS in ethanol stock solution. After approximately 1 hour had passed, allowing time for the MPTMS molecules to assemble into a monolayer on the ends of the gold nanorods, 125μL of water and 125μL of 2 M ammonia was added to the cuvette which was then capped and mixed by three successive inversions. The assembly of the MPTMS monolayer on the ends of the gold nanorods as well as the subsequent end-to-end assembly of the gold nanorods was monitored continuously by UV-Vis spectroscopy.

- Gold Nanorods Encapsulated in a Thin Silica Shell: The encapsulation of gold nanorods with a silica shell was performed in an ethanol and water mixture. 1 ml of PVP stabilized gold nanorods was mixed with 10μL of a

6.96mM MPTMS in ethanol stock solution in a cuvette. After approximately 1 hour had passed, allowing time for the MPTMS molecules to assemble into a monolayer on the ends of the gold nanorods, excess MPTMS in solution was removed by centrifugation of the sample at 8500 RPM for 30 minutes and the nanorods were re-dispersed into water.

Following the functionalization of the gold nanorods with MPTMS and their purification, sodium metasilicate was used to deposit a shell of silica using two different methods. 500µL of the sample was used for the first method based on slow coating of silica and the remaining 500µL was used for the rapid precipitation of silica.

To the 500µL of purified MPTMS functionalized gold nanorods dispersed in water, approximately 725µL of a sodium metasilicate in water stock solution with a concentration of 0.354 mg/ml was added[84]. This amount was selected to provide a SiO_2 concentration that was in ten times excess to the concentration of the gold nanorods in the solution. The cuvette was then capped and inverted three times for mixing and was allowed to sit overnight. On the following day the UV spectrum of the sample was recorded and a TEM grid of the sample was prepared.

- Gold Nanorods End Functionalized with Silica: 500µL of the purified MPTMS functionalized gold nanorods in water were used. To this

amount, 725μL of a sodium metasilicate in water stock solution with a concentration of 0.354mg/mL was added[84]. Additional experiments producing better end-functionalized gold nanorods were also performed with 0.177mg/mL and 0.089mg/mL sodium metasilicate stock solutions. This mixture was then transferred to a scintillation vial were 5mL of ethanol was added under vigorous mixing by a vortex mixer. 1mL of this sample was then withdrawn and placed in a cuvette and UV spectra were collected every 5 minutes. After approximately one hour, a TEM grid of the sample was prepared.

- Characterization: UV-Vis spectra were recorded using a V-530 spectrophotometer (Jasco Inc., MD). TEM images were recorded by a FEI Morgagni 268D operated at an accelerating voltage of 60 kV. Samples for TEM analysis were prepared by placing drops of colloidal solution on Formvar carbon coated copper grids (Electron Microscopy Sciences, PA). The colloidal solution was allowed to stand on the grid for 1 minute following which the extra solution was removed using a Kimwipe as blotting paper. The solvent was drawn from the side of the grid to prevent disruption of the sample leaving a thin layer of solvent to evaporate.

3.2.2 Results and Discussion

Figure 3.8 shows a proposed schematic of gold nanorods assembled by silica. In this method of assembly, MPTMS molecules are first functionalized onto the ends of the gold nanorods followed by the condensation of the silane groups into bulk SiO_2. The self condensation of the silane groups in the resulting composite mediates the end-to-end linking of gold nanorods.

The successful functionalization of gold nanorods by MPTMS is confirmed by the UV spectrum before and after the functionalization (Figure 3.9a and 3.9b). The red-shift that is observed is indicative of the functionalization of the gold nanorod with a material that increases the dielectric constant of the environment surrounding the nanorods[16, 35, 36]. Following the functionalization of the gold nanorods, a small amount of water and ammonia is added to the cuvette to raise the pH and initiate the condensation polymerization of the silane groups[82]. The reaction is recorded as a function of time though various UV spectra collected throughout the reaction (Figure 3.9 curves c-l). The formation of an isobestic point and development of red-shifted in the longitudinal resonance indicates that uniaxial plasmon coupling is occurring between gold nanorods[61, 79]. However, the representative TEM images in Figure 3.10 do not depict only linear chains. The resulting arrays of gold nanorods are connected at the ends, as suggested by the plasmon coupling observed in the UV spectra, but multi-dimensional clusters are clearly evident rather than one-dimensional chains. While this assembly needs to be refined further, it raises the question of using gold nanorods functionalized with MPTMS to direct the growth of silica on the

nanorods. Such gold-silica composites would allow us to leverage the extensive knowledge in controlling the surface functionalization of silica.

The first attempt to end functionalize gold nanorods with silica was to use a sodium metasilicate solution, which is an approach that is adapted from previous studies[85, 86]. It was believed that the silane groups on the MPTMS functionalized gold nanorods would act as sites of nucleation for silica growth. Following the functionalization with MPTMS, the gold nanorods were centrifuged to remove excess MPTMS and then re-dispersed in water. Since the metasilicate deposition occurs at an extremely slow rate, the entire gold nanorod was covered with a thin and smooth layer of silica. The length of time and concentration of metasilicate could be altered to control the thickness of the coating applied. The silica coating was confirmed by a significant red-shift of the longitudinal peak in the UV spectrum of the sample as shown in Figure 3.11. A TEM image of the sample shows the thin layer of silica deposited onto the surface of the gold nanorods.

In a second method of silica deposition onto the ends of gold , the rapid precipitation of silica was forced by changing solvent mixing ratios[84, 87]. In this procedure, gold nanorods functionalized with MPTMS were transferred into water and a metasilicate solution was used to begin silica deposition as before. After the addition of the metasilicate solution a large volume of ethanol was added to the mixture. As the metasilicate is relatively insoluble in this water-ethanol mixture, the rapid precipitation of silica occurs. Using this procedure it was found that the silica deposited preferentially towards the ends of the nanorods. A

possible explanation for this phenomenon is that during the slow deposition of silica the shell was able to grow to encompass the entire rod, whereas in the rapid deposition approach the silane groups offer the only point of nucleation and the rapid deposition does not allow time for growth of silica onto the sides of the gold nanorods. Also, as the concentration of metasilicate used in the procedure was decreased, both the number of gold nanorods with silica coating on the sides as well as the thickness of the side coating decreased. Figure 3.12 shows a TEM image of the sample. The silica groups tend to be located as irregular clusters near the ends of the gold nanorods. While some silica is still deposited on the sides of the rods, the continued refinement of this approach offers promise in the development of silica end-functionalized gold nanorods.

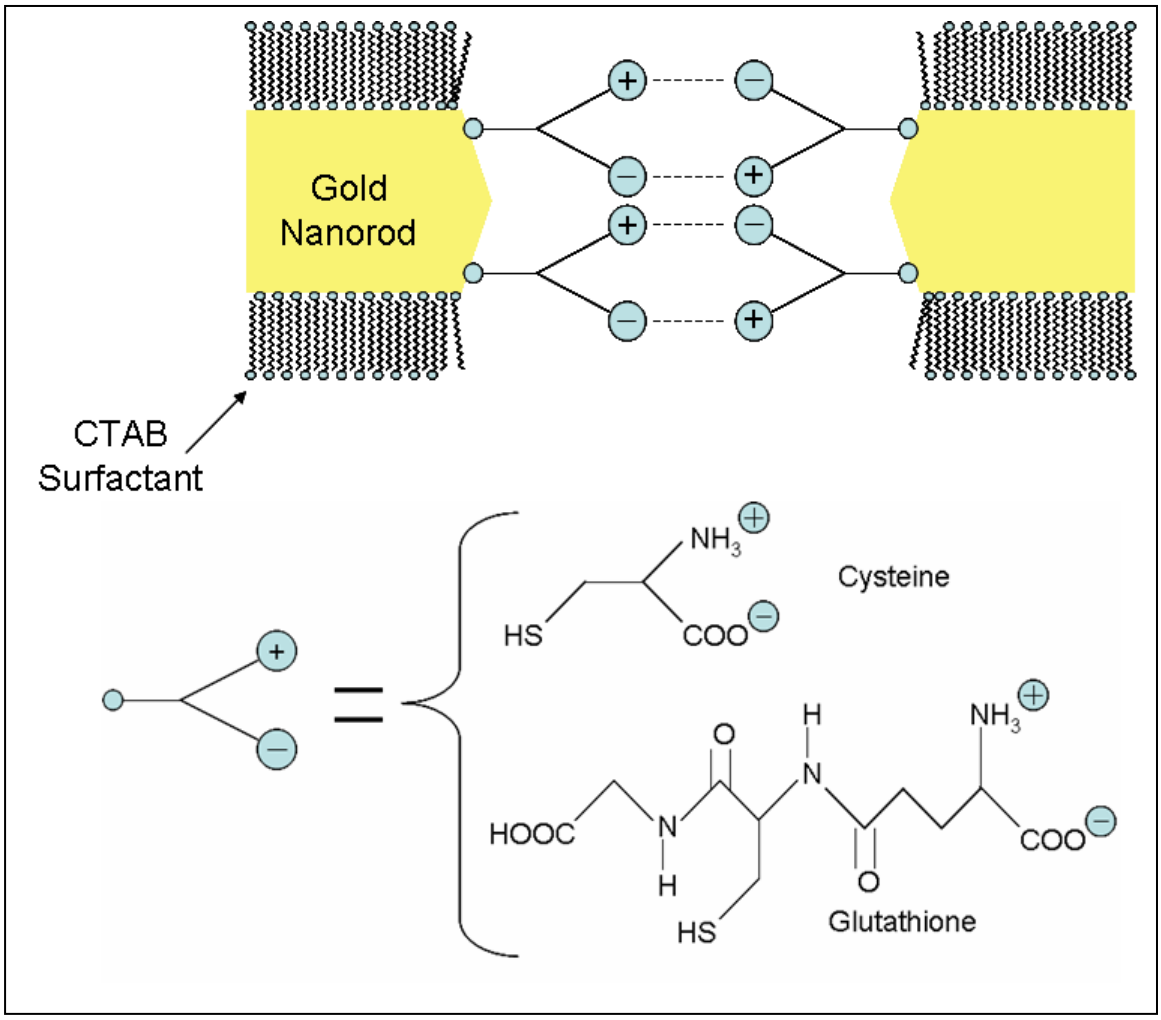

Figure 3.1: Schematic of Self-Assembly Using Cysteine and Glutathione

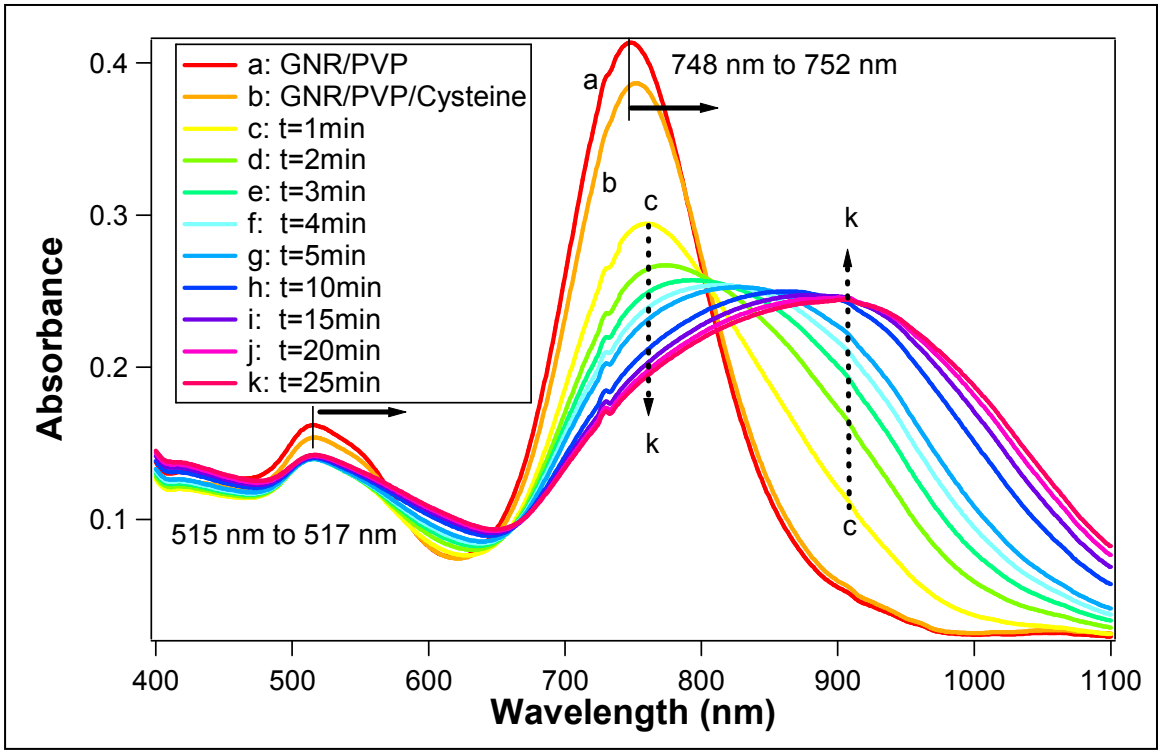

Figure 3.2: Optical Spectra of Gold Nanorods Self-Assembled Using Cysteine

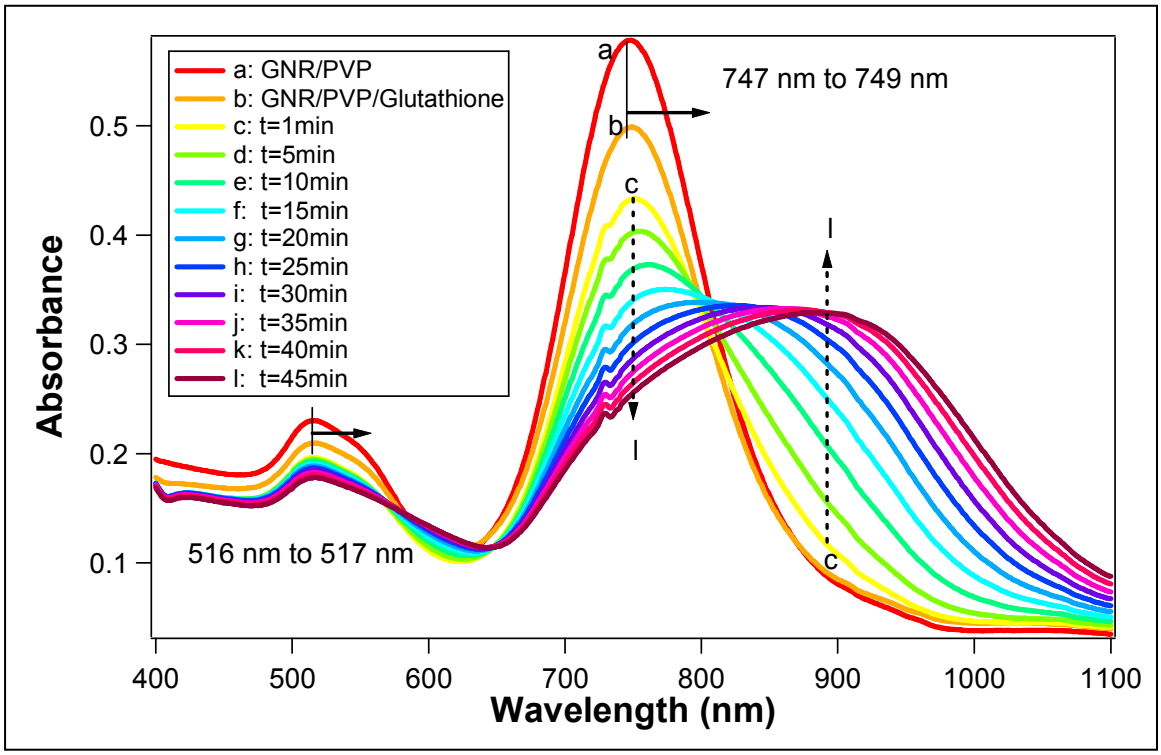

Figure 3.3: Optical Spectra of Gold Nanorods Self-Assembled Using Glutathione

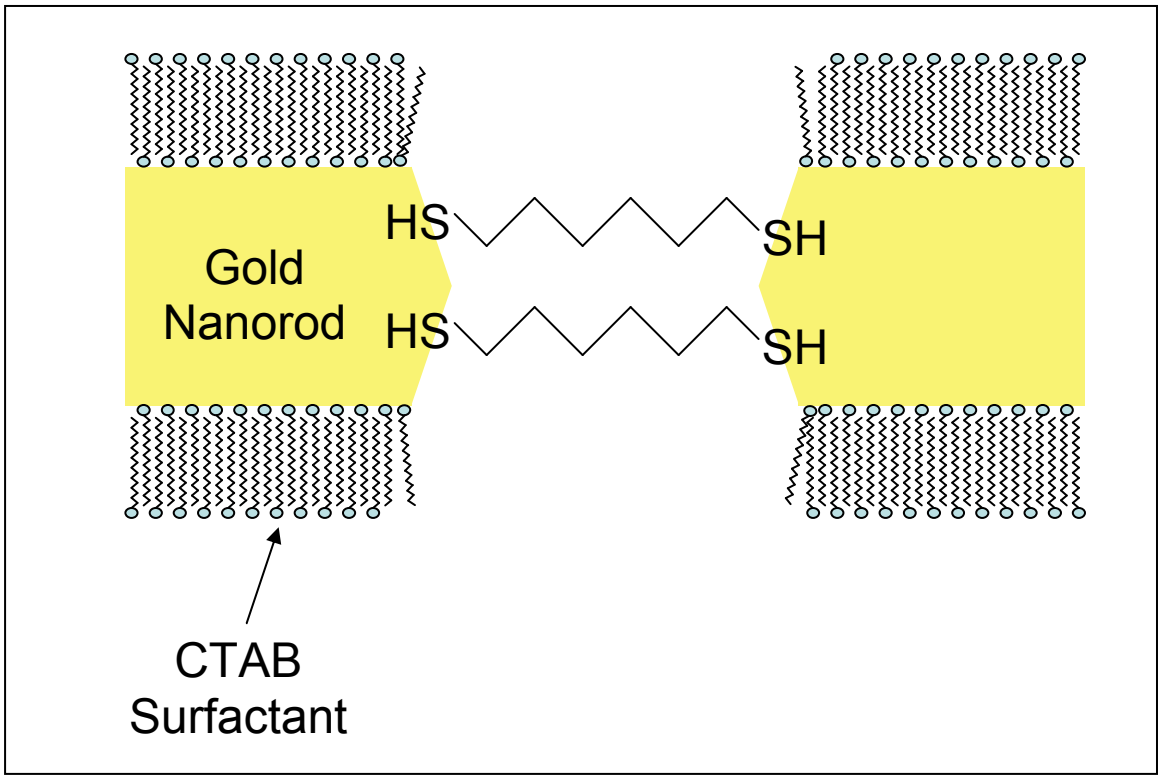

Figure 3.4: Schematic of Self-Assembly of Gold Nanorods Mediated by 1,6-Hexanedithiol

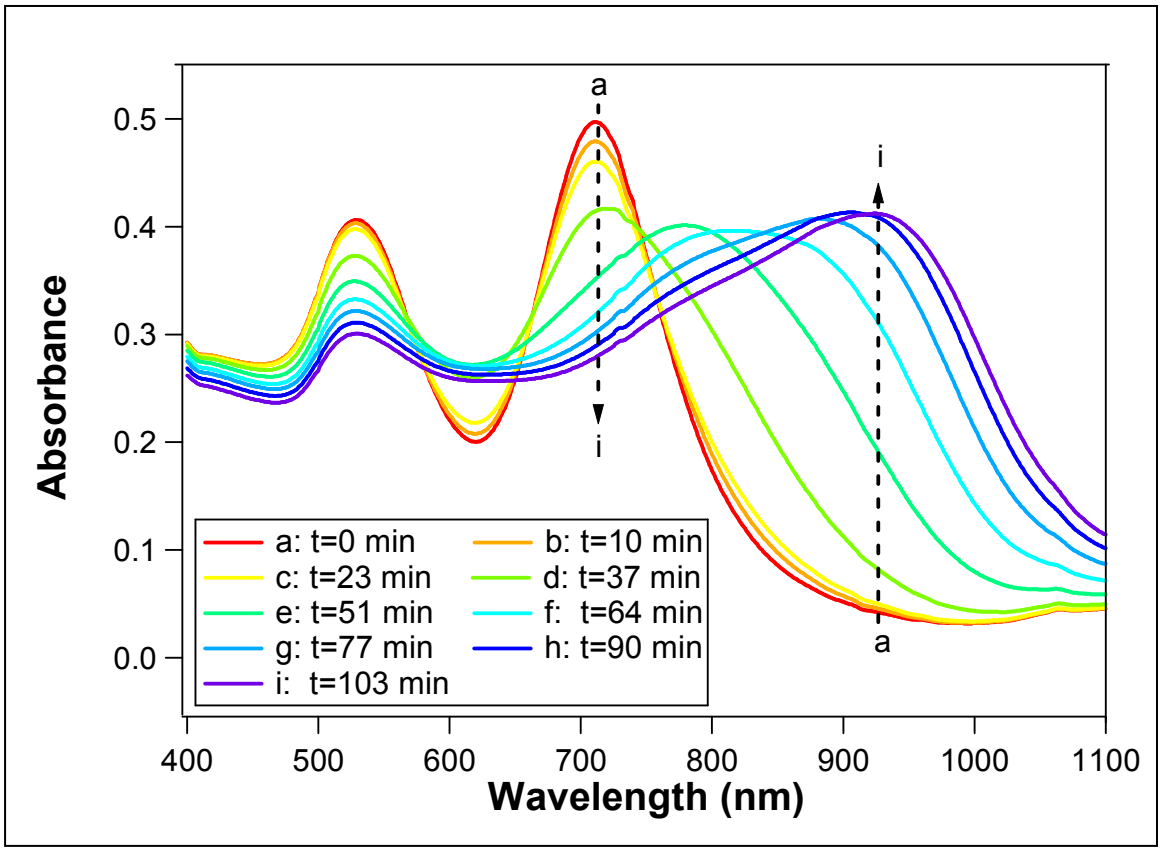

Figure 3.5: Optical Spectra of Gold Nanorods Self-Assembled Using 1,6-Hexanedithiol

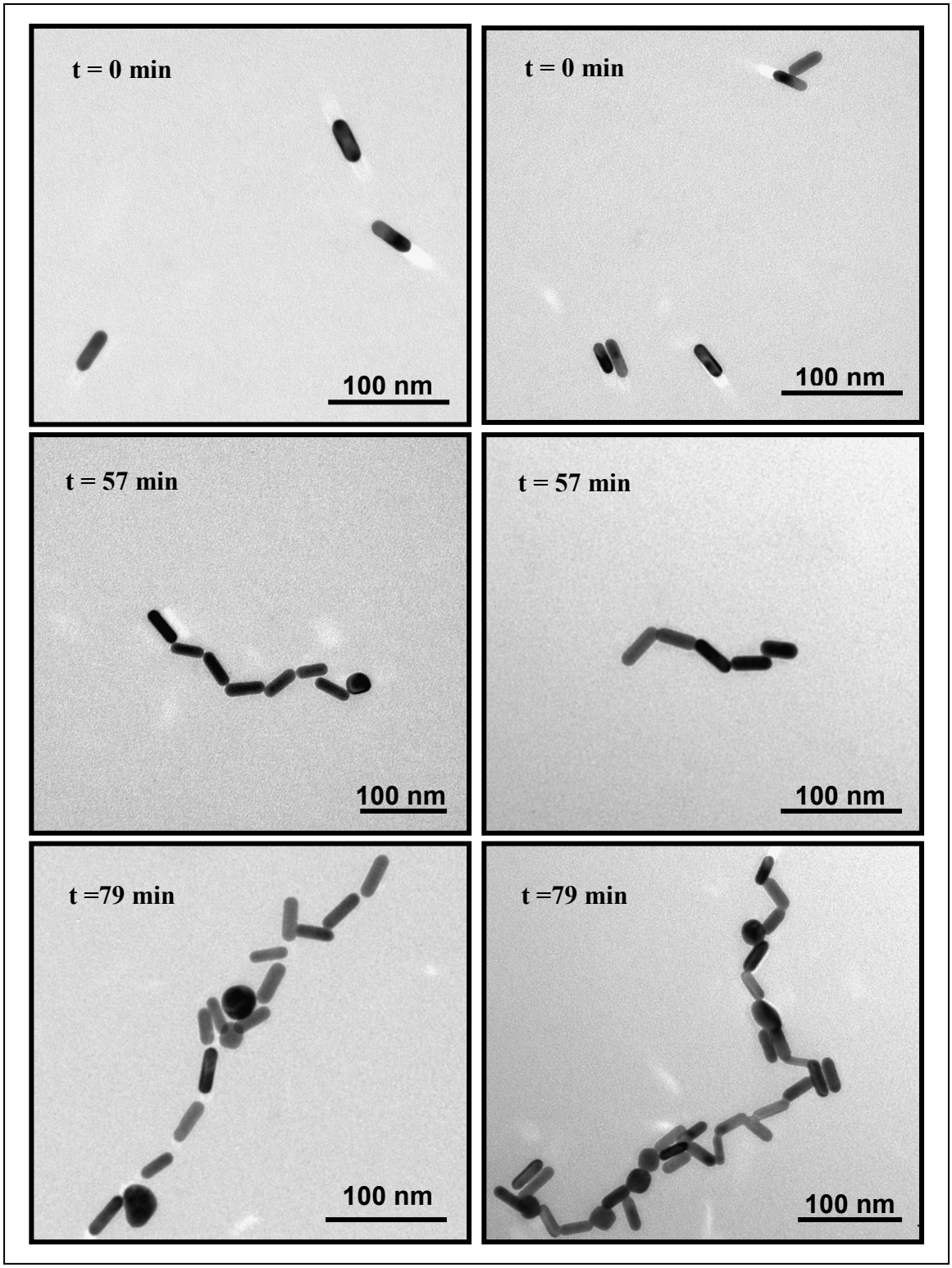

Figure 3.6: TEM Images of Self-Assembly of Gold Nanorods Using 1,6-Hexanedithiol

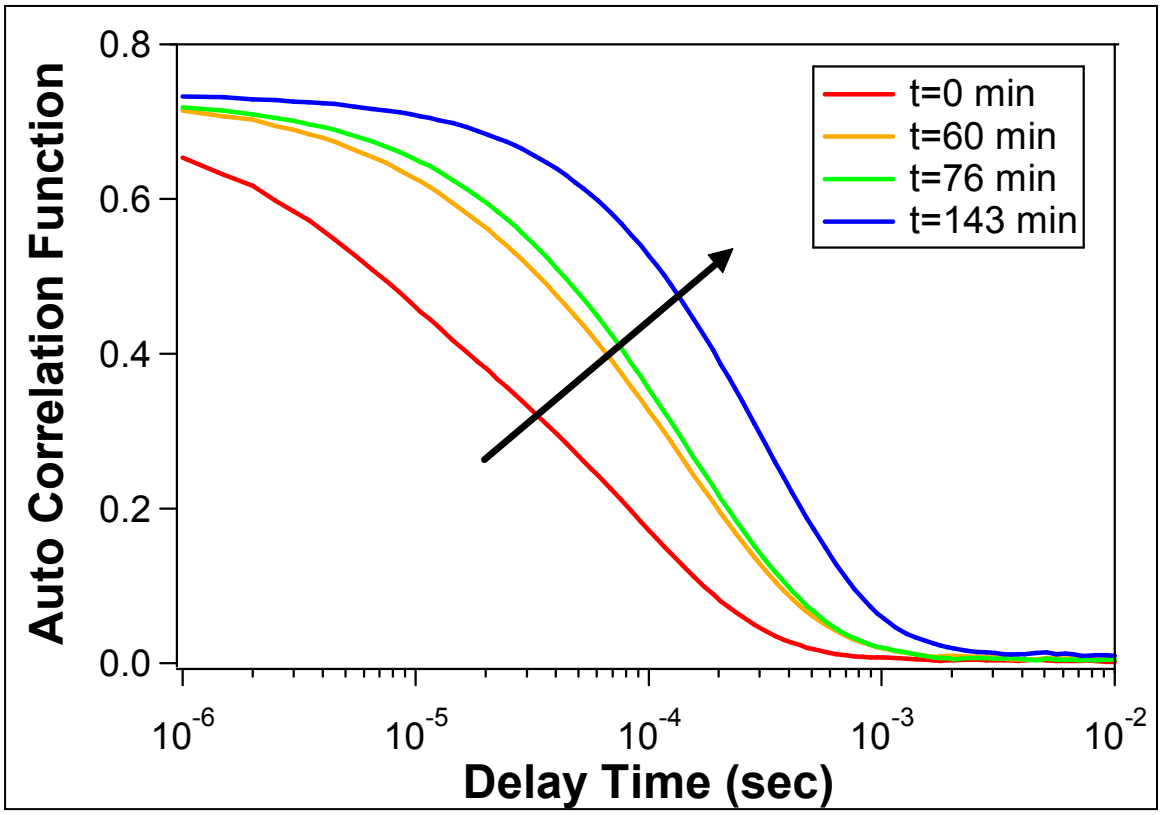

Figure 3.7: Intensity Autocorrelation in DLS Characterization of Gold Nanorod Assembly Using 1,6-Hexanedithiol

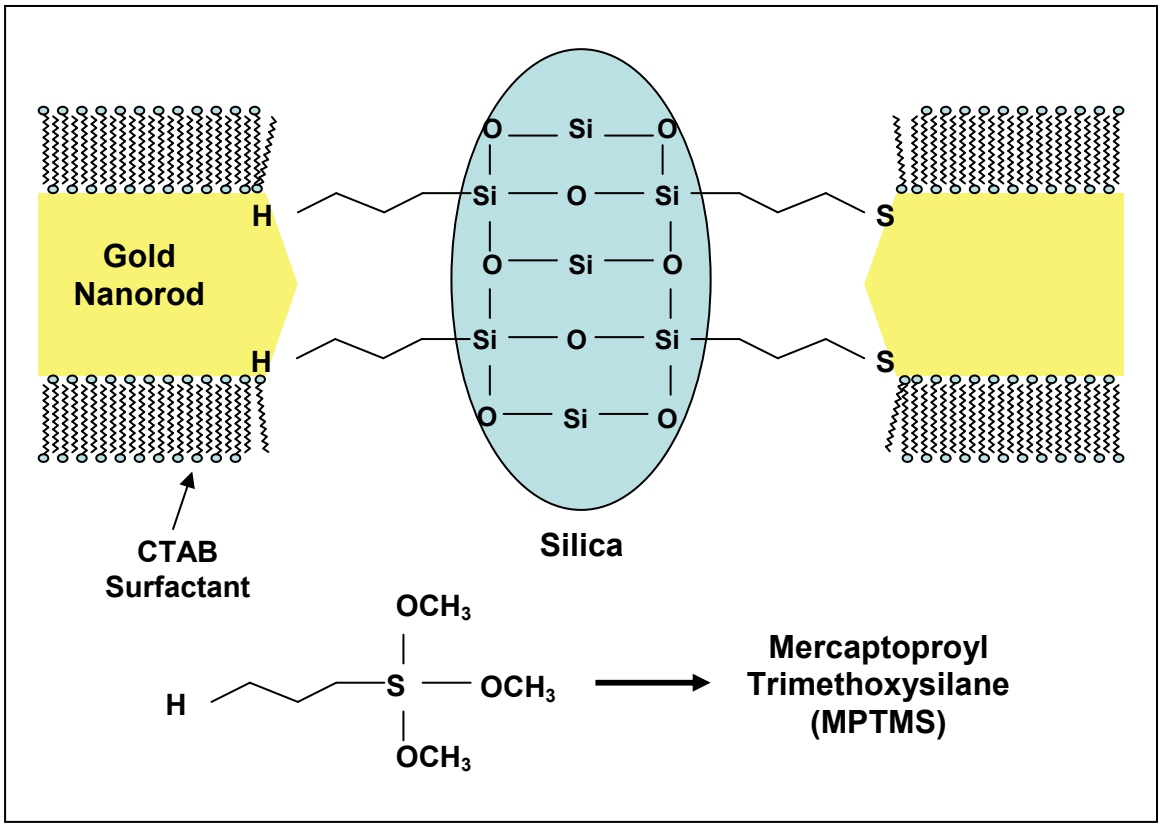

Figure 3.8 Schematic of Self-Assembly of Gold Nanorods Mediated by MPTMS by MPTMS Functionalization and Condensation of Silica

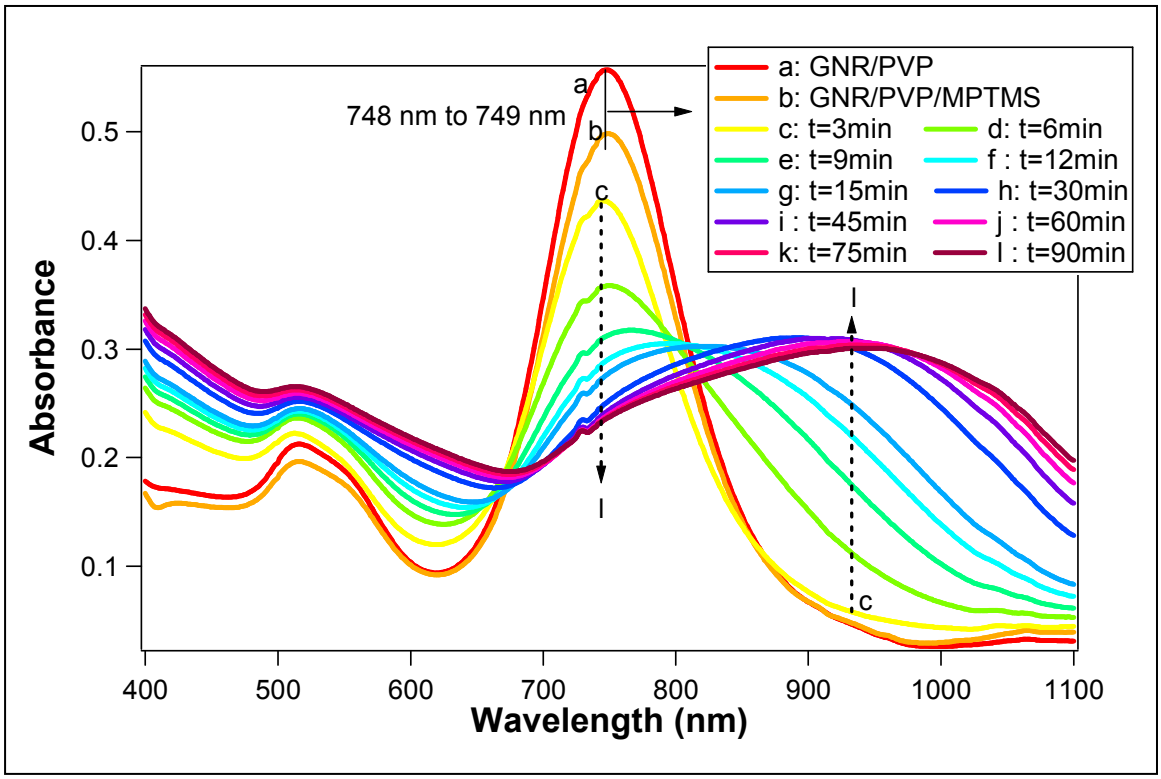

Figure 3.9: Optical Spectra of Gold Nanorods Self-Assembled Using MPTMS

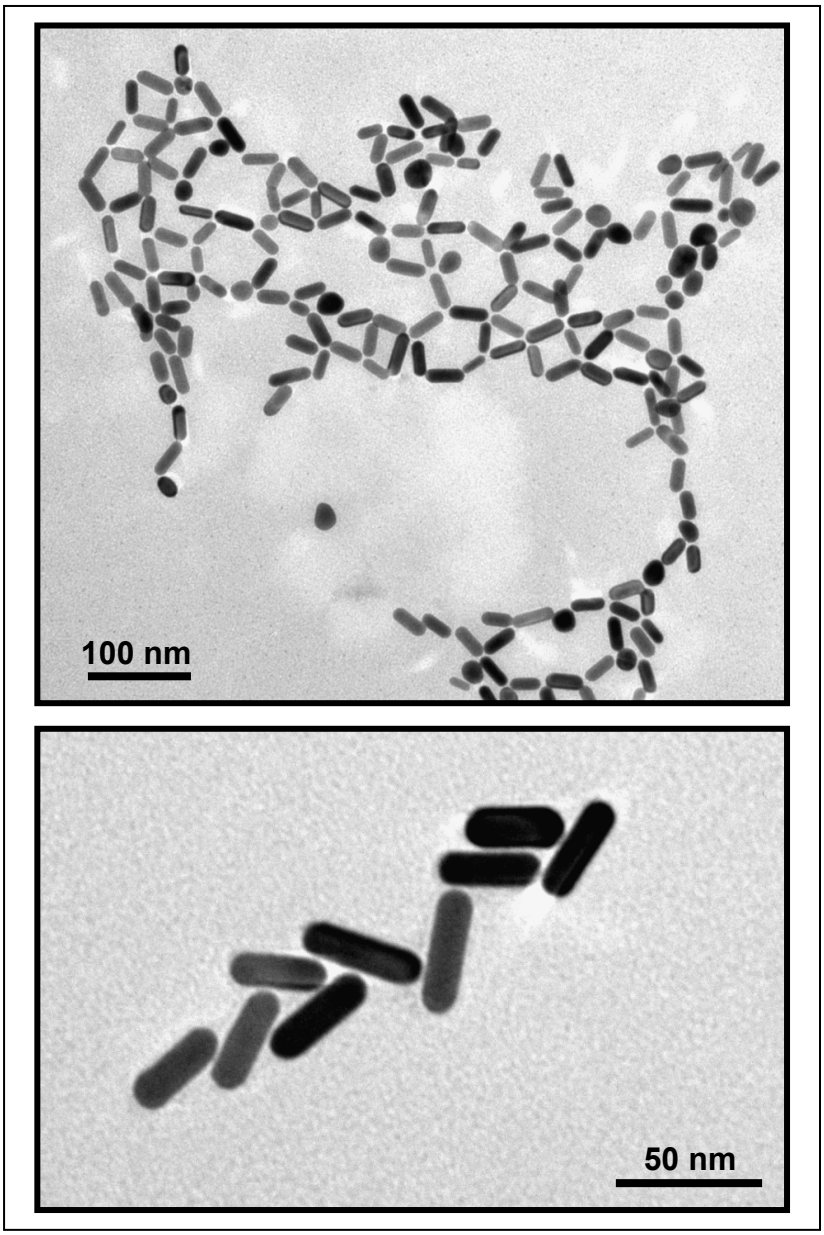

Figure 3.10: TEM Images of Gold Nanorods Assembled Using MPTMS

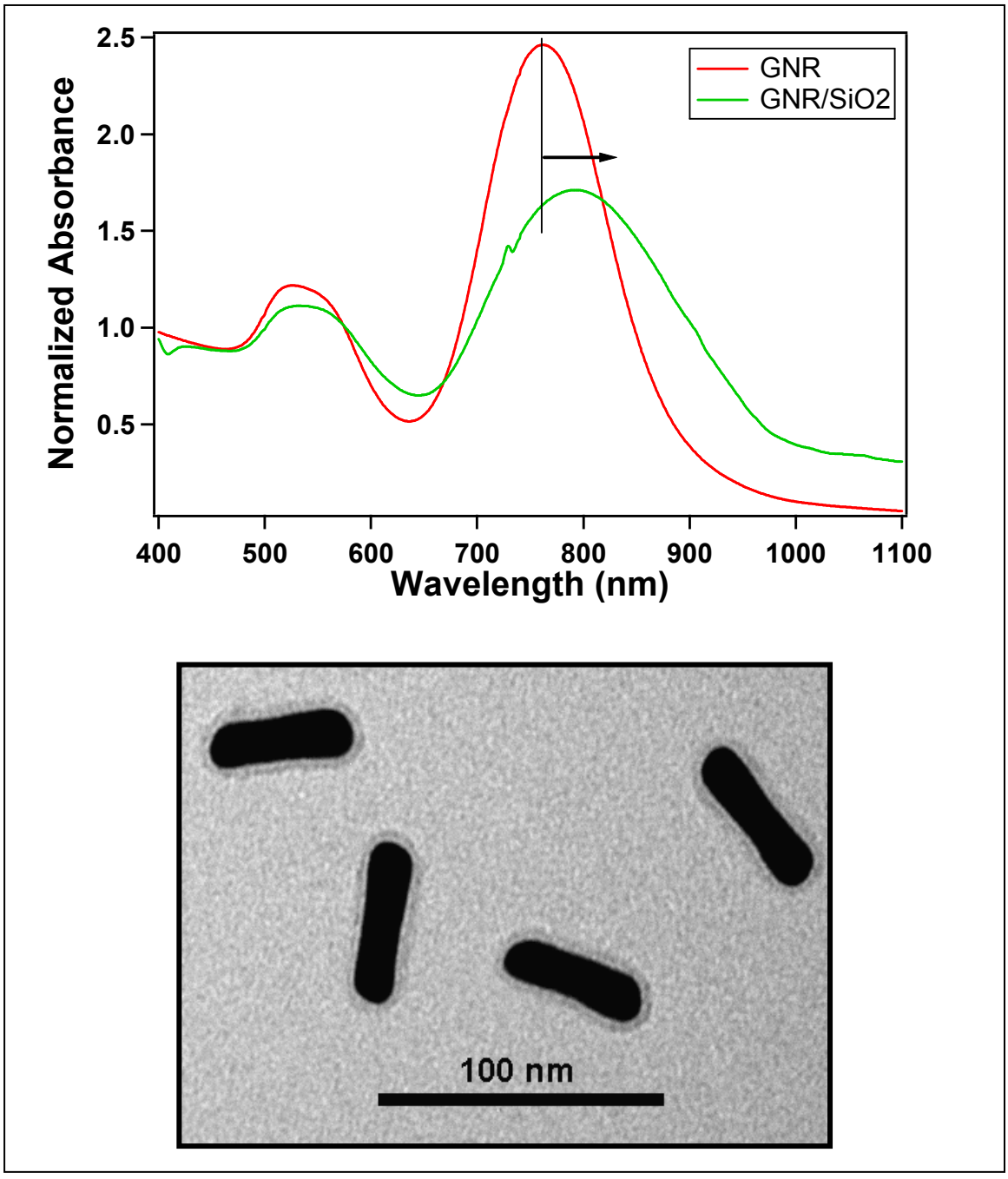

Figure 3.11: Optical Spectra and TEM Image of Gold Nanorods Encapsulated with Thin Silica Shell

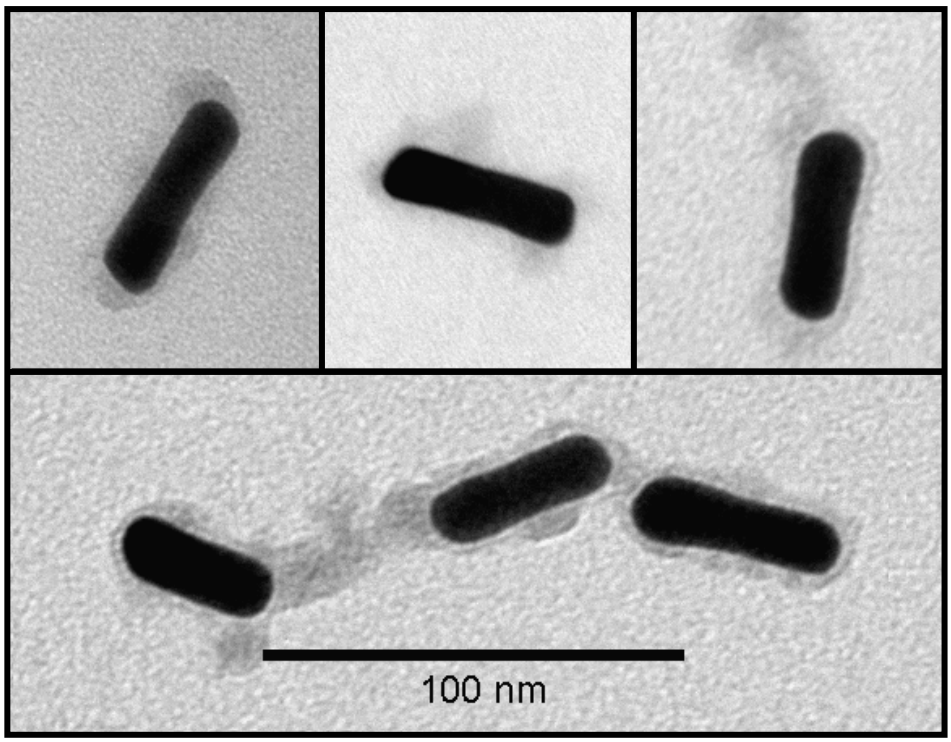

Figure 3.12: TEM Images of Gold Nanorods End-Functionalized with Silica

CHAPTER FOUR: REVERSIBLE ASSEMBLY OF GOLD NANORODS USING A RESPONSIVE POLYPEPTIDE

While the directed irreversible assembly of gold nanorods examined in Chapter Three forms an important accomplishment, principles for controlled reversible self-assembly of gold nanorods are highly desirable in bottom-up creation of nanostructures. This chapter focuses or assembling gold nanorods in an end-to-end fashion through the use of a responsive polypeptide. The polypeptide undergoes a secondary conformational change based on the pH of its surrounding environment. By functionalizing the gold nanorods with a disulfide modified polypeptide, this conformational change can be exploited to trigger end-to-end assembly or dispersion of the gold nanorods, which provides a powerful and novel means towards reversible self-assembly of nanoparticles.

4.1 Experimental

- Materials: A disulfide modified γ-benzyl-L-glutamate (SSPLBG), with M_w~27000, available in our laboratory (courtesy: doctoral work of Dr. Alved Williams) was used. The SSPBLG was converted into a disulfide modified poly(L-glutamic acid) (SSPLGA) through a debenzylation reaction using HBr/AcOH (courtesy: Dr. J.-Y. Shim). The detailed

preparations of SSPLBG and SSPLGA have been reported elsewhere[88, 89]. The preparation of gold nanorods stabilized by PVP in ethanol that are functionalized with SSPLGA has been described in Chapter Two. NaOH (certified ACS grade) was purchased from Fisher Scientific and HCl (37% reagent grade) was purchased from Sigma Aldrich. Water used for all synthesis was purified using an EasyPure™ UV system (Barnstead, IA). A 0.2 μm filter incorporated into this system was used to remove any particulate matter.

- Functionalization of Gold Nanorods with SSPLGA: In a scintillation vial 1mL of concentrated PVP stabilized gold nanorods in ethanol were diluted to a volume of 5mL through the addition of an additional 4mL of pure ethanol. Under a gentle vortex mixing, 30μL of 1mg/mL SSPLGA aqueous stock at a pH of 4 was added to the scintillation vial. Following mixing, the scintillation vial was allowed to rest for a period of 24 hours to allow an adequate amount of time for the self-assembly of the SSPLGA monolayer onto the ends of the gold nanorods.

- End-to-End Assembly and Disassembly of SSPLGA Modified Gold Nanorods: To assemble the SSPLGA modified gold nanorods in an end-to end fashion 1mL of SSPLGA modified gold nanorods were measured into a cuvette. To this sample, 1mL of water at an elevated pH (pH~9.5) was added to the cuvette. Once the water was added, a small quantity

(<10μL) of 0.1 M NaOH was used to raise the pH (pH~11.5) to ensure the gold nanorods begin in a properly dispersed state. To trigger the end-to-end assembly a few drops (~20μL) of 0.1 M HCl were used to lower the pH (pH~3.5) and caused a vivid color change from pink to blue. To reverse the assembly and regain the color of the solution a few drops (~20μL) of 0.1 M NaOH were used to increase the pH (pH~11.5). Through these acid and base additions the sample can be altered between the assembled state (low pH) and disassembled state (high pH) repeatedly. UV-Vis spectra and DLS autocorrelation functions were collected at each step of the process along with corresponding TEM grids during the cycling between the assembled and disassembled states.

- Characterization: UV-Vis spectra were recorded using a V-530 spectrophotometer (Jasco Inc., MD). Dynamic light scattering (DLS) measurements were performed at 20^{o}C using a Zetasizer Nano-S (Malvern Instruments, PA) which was equipped with a red laser (633 nm) and a detector for analyzing backscattering at 173^{o} from the incident light. All pH measurements were performed using an Accumet electrode from Fisher Scientific (Catalog Number 13-620-290) attached to a Cole-Palmer pH/mV/^{o}C bench top meter (Model Number 59003). TEM measurements were performed on a FEI Morgagni 268D operated at an accelerating voltage of 60 kV. Samples for TEM analysis were prepared by placing drops of colloidal solution on Formvar carbon coated copper grids

(Electron Microscopy Sciences, PA). The colloidal solution was allowed to stand on the grid for 1 minute following which the extra solution was removed using a Kimwipe as blotting paper. Most of the solvent was drawn from the side of the grid and the residual thin layer of solvent was left to evaporate.

4.2 Results and Discussion

SSPLGA undergoes a conformational change with pH, as shown in Figure 4.1, which can be exploited for end-to-end linking. The general concept has been recently utilized to aggregate and disperse gold nanoparticles[88]. In that research it was shown that at a high pH the polypeptide is in a de-protonated, random coil state while at low pH the SSPLGA molecule changes to a helical conformation with strong hydrophobic interactions as well as dipole-dipole interactions. The prior study[88] has reported IR spectra to show that the SSPLGA monolayer undergoes a conformational change on gold surfaces in reaction to bulk pH change as well as literature data on molar enthalpy of hydrogen bonding, specific optical rotation, and ionization for the helix-coil transition of PLGA to show that the aggregation of the SSPLGA modified gold nanoparticles corresponds to the conformation change in the secondary structure of the polypeptide.

Figure 4.2 shows the UV spectra of the gold nanorods stabilized with PVP prior to and following the functionalization with SSPLGA in an ethanolic environment. After modification with the SSPLGA, a red-shift of 1 nm is

observed in the transverse and longitudinal resonances due to the minor change in the dielectric environment of the gold nanorod[16, 35, 36] from the presence of the polypeptide on the ends of the particle. To leverage the pH induced transition in the conformation of the SSPLGA molecules, a slight amount of water was added to the colloidal solution. Figure 4.2 shows that a small blue-shift occurs due to the decrease in the refractive index of the fluid medium[16, 35, 36].

The reversible end-to-end assembly process, as shown in Figure 4.3, is driven by a change of pH which induces a conformational change in the SSPLGA molecules located on the ends of the gold nanorod. When the pH of the solution is lowered to ~3.5, both the transverse and longitudinal peaks shift to higher wavelengths (Figure 4.4) due to plasmon coupling occurring between the particles which is indicative of the end-to-end linking[61, 79]. The magnitude of the shift is quite large at approximately 45 nm for the longitudinal peak. Because the direction and magnitude of the shift in the longitudinal resonance is highly sensitive to the style of the linking (axial or side-to-side), the observed red-shift indicates that end-to-end linking is occurring[90]. As seen in Figure 4.4, the shift in the optical spectrum can be oscillated between the two states when the pH is increased and then lowered again. The reversible nature of this process can be seen in Figure 4.5 where the shift in the longitudinal resonance is shown as a function of changes in pH over multiple cycles. Corresponding TEM images shown in Figure 4.6 show the dispersed state of the gold nanorods functionalized with SSPLGA prior to assembly (Figure 4.6a) and the end-to-end linked state at low pH (Figure 4.6b-d). The images reveal that nanostructures containing four to

eight linked gold nanorods in length with a few large aggregates also being present. The linking is not entirely end-to-end as some side-to-side interactions are observed in the images. However, TEM images only provide a selective snapshot of the chains after a drying process in which aggregation of chains can occur. Since the optical spectra shown in Figure 4.4 for the low pH state in solution show a red-shift in the longitudinal resonance, we believe that a majority of the nanostructures in the solution are end-to-end linked gold nanorods.

The changes shown in figure 4.4 and 4.5 occur within a few minutes of cycling the pH, which is consistent with the past study on gold nanoparticles[88]. The reversible response shown here is an interesting contrast to the assembly of gold nanorods into rings using solvent quality changes where the assembly process requires long times (~hours) and significant changes in the volume of the solvent mixture (~5-35% v/v). The optical shift in the longitudinal resonance with gold nanorods modified with SSPLGA is similar to the results found when the end-to-end assembly was driven by hexanedithiol and is also consistent with past experimental[21, 28, 30, 59-61, 63] and theoretical studies[90]. However, unlike Figure 3.5 in the hexanedithiol mediated assembly process, the transverse peak in Figure 4.4 shows a slight broadening and growth of a shoulder around 600 nm when the pH is lowered and these changes are reversible. This change in the transverse resonance is inconsistent with the one-dimensional assembly of gold nanorods in the axial direction as no shift in the transverse peak should be observed for end-to-end linking. Past studies that have probed end-to-end linking of gold nanorods using small molecular weight compounds have not seen shifts in the transverse

resonance. Only the report by Mann and co-workers[77] has shown a red-shift in the transverse resonance along with a blue-shift in the longitudinal resonance, which are the expected results of side-to-side assembly of gold nanorods that were observed in their study. We believe that at low pH environments SSPLGA mediates aggregation of the gold nanoparticles in the samples, which can occur in the surfactant method of gold nanorod preparation. Aggregation of these isotropic contaminants is manifested as the shoulder at 600 nm in the UV spectra but has no observable effect in the region around 700-800 nm where only the contribution from the anisotropic gold nanorods is observed.

The DLS autocorrelation function of the samples in the assembled (high pH) and unassembled (low pH) states for the first two cycles are shown in Figure 4.7. As in the case of the end-to-end linking with hexanedithiol, the decay of the autocorrelation function shifts to longer times when the gold nanorods are linked. However, unlike the hexanedithiol scenario, increasing the pH disperses the gold nanorods resulting in a faster decay corresponding to larger diffusion coefficient. Since intensity scattering in DLS measurements is significantly more sensitive to size polydispersity than the optical absorption spectra, the results in Figure 4.7 demonstrate the effectiveness of using the SSPLGA conformational change to reverse the end-to-end linking. It can be observed from the changes in the autocorrelations function that the overall size of the gold nanorod complex might not completely return to there original state. This scenario is also suggested by slight irreversibilities in the longitudinal resonance shift after many cycles as shown in Figure 4.5.

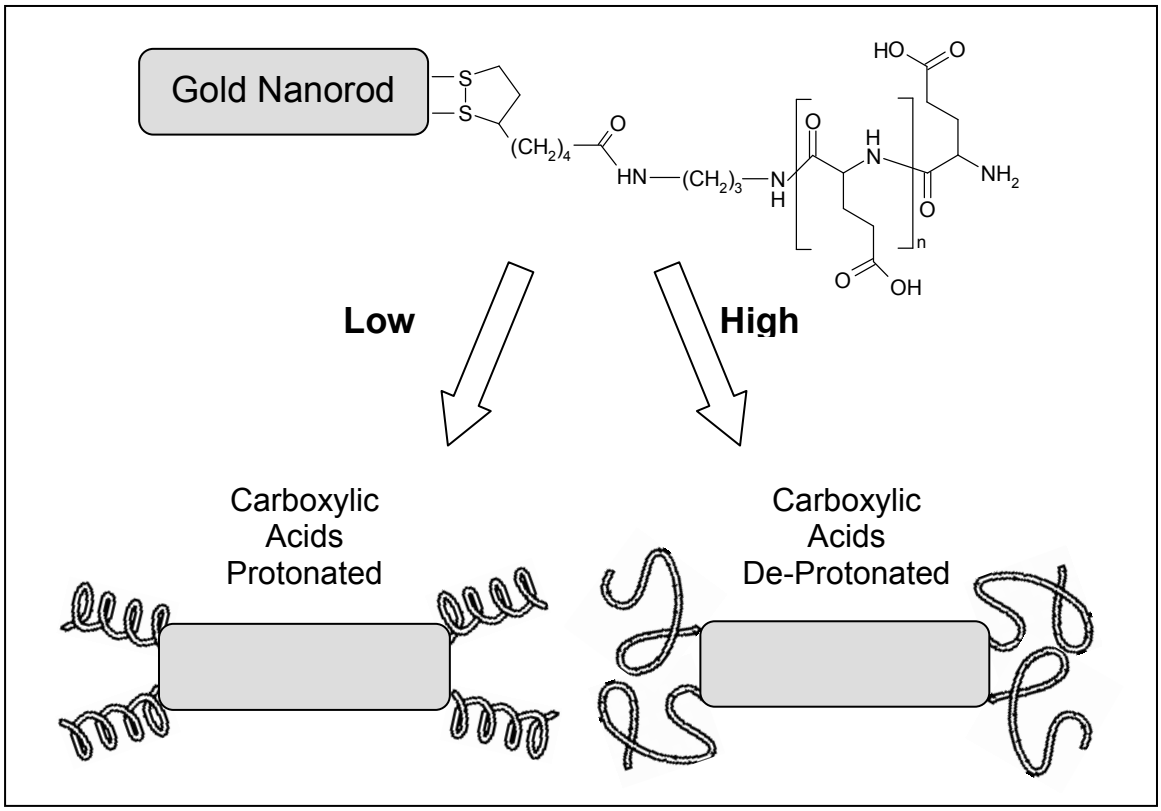

Figure 4.1: Schematic of Gold Nanorods Modified with SSPLGA

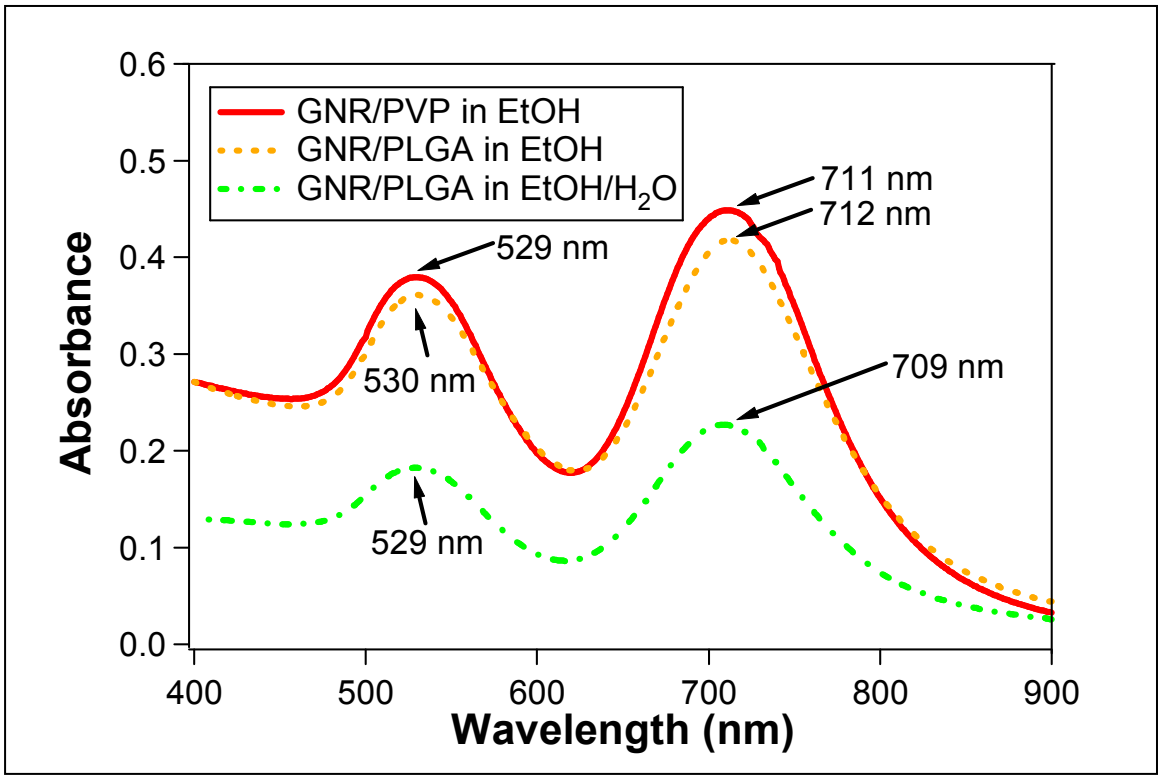

Figure 4.2: Optical Spectra of Gold Nanorods Modified with SSPLGA

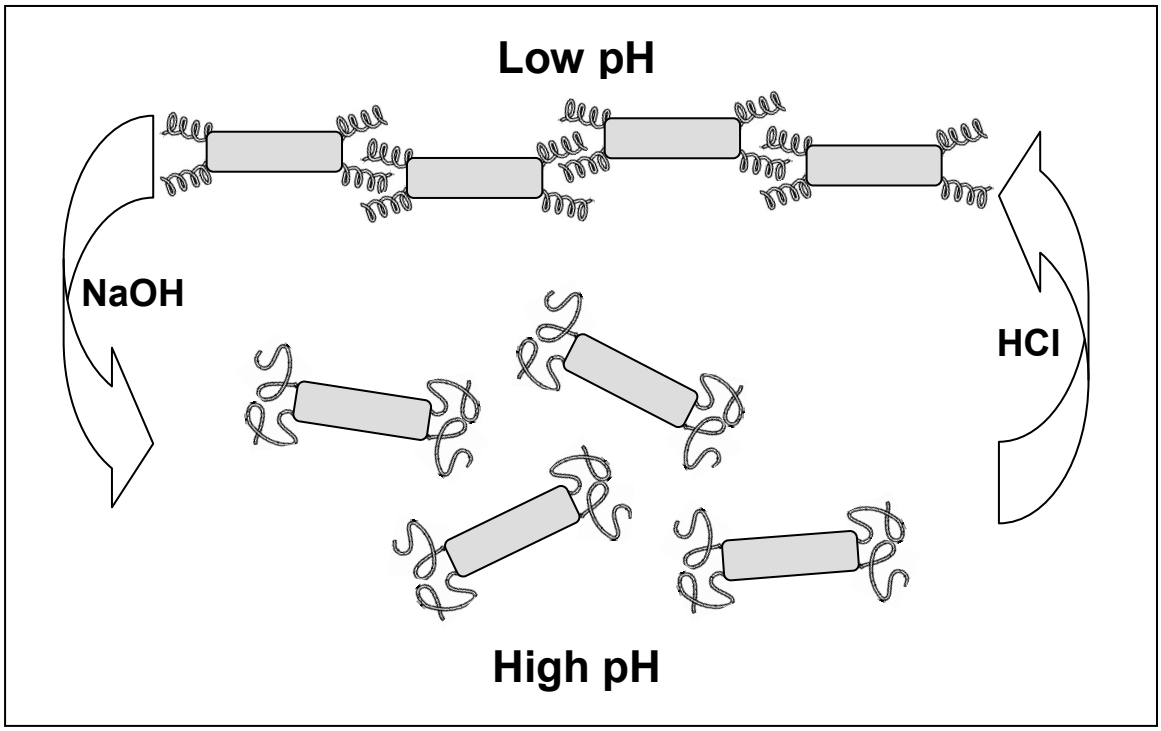

Figure 4.3: Schematic of End-to-End Assembly of SSPLGA Modified Gold Nanorods

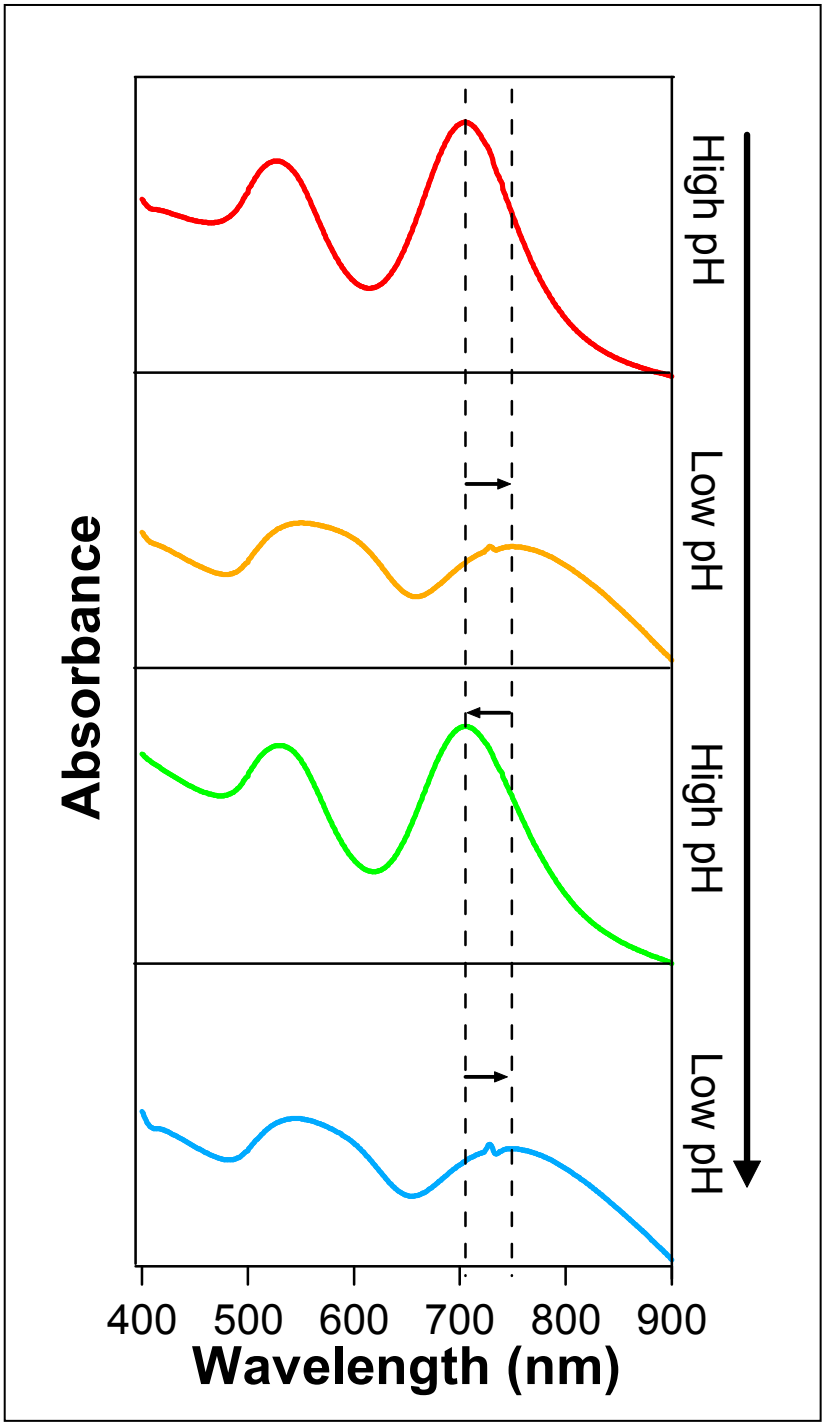

Figure 4.4: Optical Spectra of End-to-End Assembly and Disassembly of SSPLGA Modified Gold Nanorods

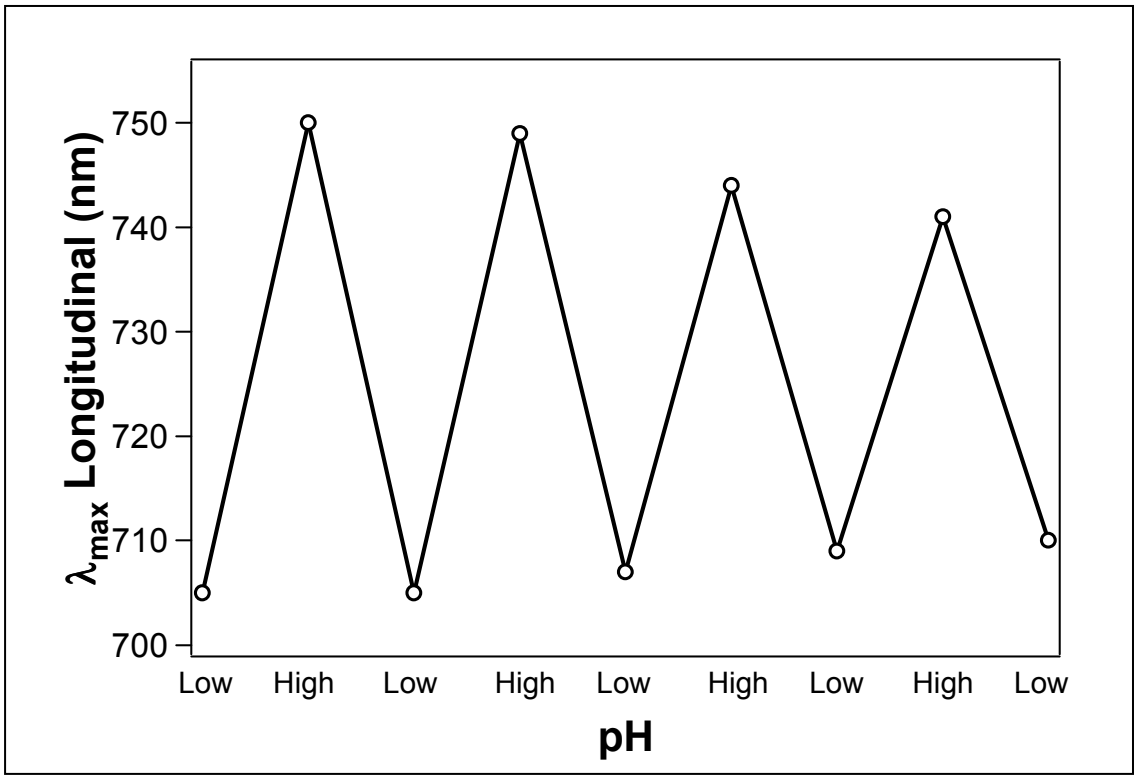

Figure 4.5: Shift in the Longitudinal Resonance During End-to-End Assembly and Disassembly of SSPLGA Modified Gold Nanorods

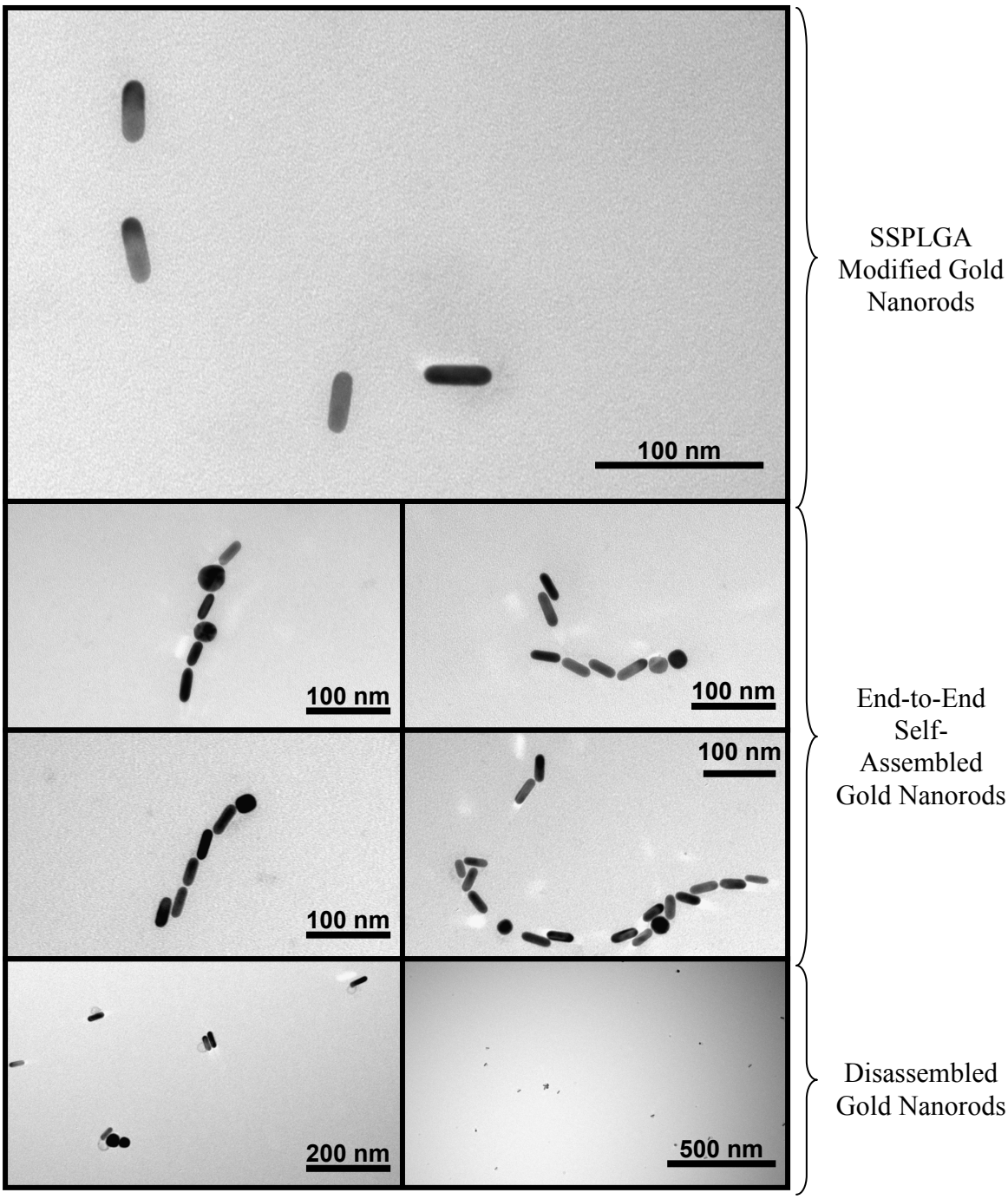

Figure 4.6: TEM Images of End-to-End Assembly and Disassembly of SSPLGA Modified Gold Nanorods

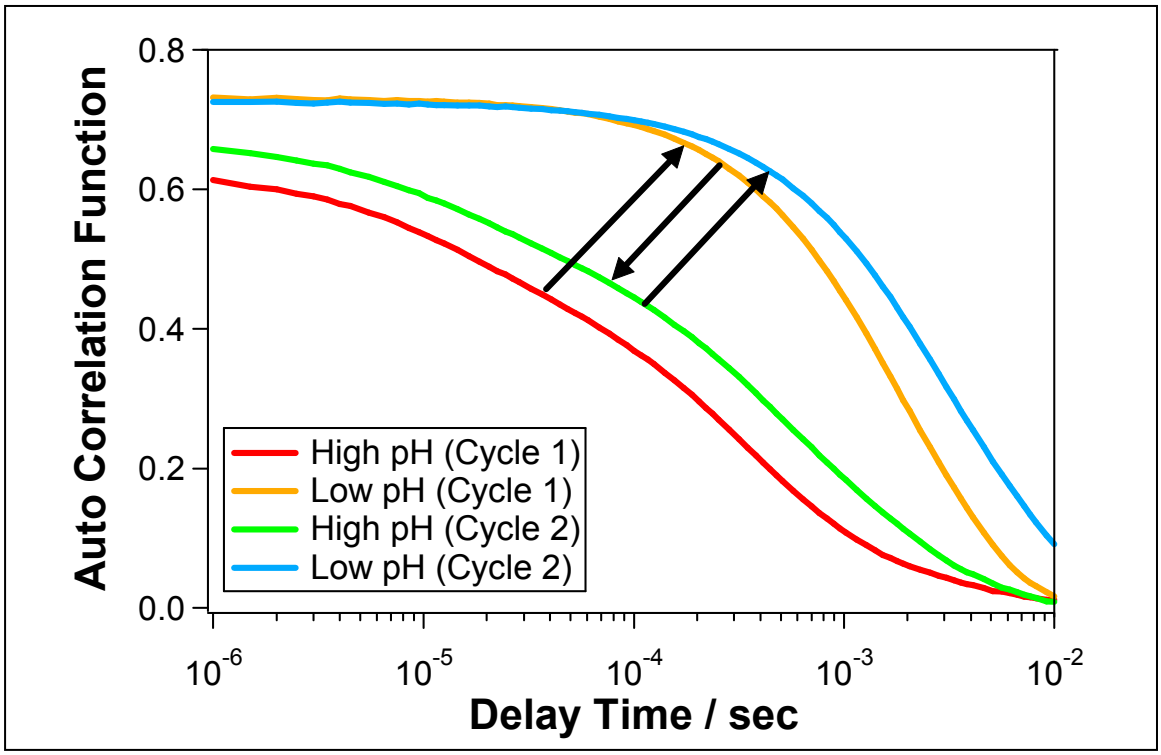

Figure 4.7: Intensity Autocorrelation in DLS Characterization of End-to-End Assembly and Disassembly of SSPLGA Modified Gold Nanorods

CHAPTER FIVE: SUMMARY, CONCLUSIONS, AND FUTURE WORK

5.1 Summary and Conclusions

In summary, the research described in this thesis has focused on the directed assembly of gold nanorods and established techniques and principles utilized to control that assembly. Gold nanorods in this work were synthesized using the seedless one-step technique, which allows the user to easily control the size of the nanorods. This research has shown that modifying the surface of the gold nanorods with polyelectrolyte layers allows for their stabilization in organic solvents. While the layer-by-layer technique used in this process allows for the deposition for multiple layers, a single layer of PVP was found to be sufficient to stabilize the nanorods in organic solvents without aggregation of the particles.

The results presented in Chapter Three have demonstrated that stabilization in organic solvents facilitates the functionalization of the gold nanorods with simple organic ligands or organic-inorganic hybrid ligands. As a result, several strategies to drive end-to-end self-assembly of gold nanorods can be pursued. In particular, it was shown that molecules such as cysteine, glutathione and hexanedithiol were successful in inducing and end-to-end self-assembly. The self-assembly was confirmed by various experimental

characterizations such as longitudinal plasmon coupling measured using UV-Vis spectroscopy, shift in decay times in the intensity autocorrelation function from DLS, and through visualization in TEM images. While end-to-end assembly using these simple organic molecules has been reported in literature, this thesis has demonstrated extension to of these techniques to gold nanorods synthesized by the one-step seedless method, gold nanorods stabilized by polymer layers and by performing the assembly in an organic environment. The results of irreversible self-assembly using cysteine, glutathione, and hexanedithiol also provide a convenient contrast to the novel reversible self-assembly explored in Chapter Four using a pH responsive polypeptide.

This thesis project has also shown that gold nanorods functionalized with an organic-inorganic hybrid molecule such as MPTMS, can be used to direct the self-assembly of the nanorods. In this process, the condensation of silane groups functionalized onto the ends of the gold nanorods resulted in the formation of complexes where the ends of the gold nanorods were linked by silica, which has not been previously reported in literature. While these complexes did not form linear chains, it has led to the use of MPTMS for the direct condensation of silica onto the ends of gold nanorods. Composite gold nanorods were formed where silica was preferentially bound to the ends of the nanorod. Such gold-silica composites will allow researchers to leverage the extensive knowledge in controlling the surface functionalization of silica.

A novel contribution of the research presented here has been the demonstration that gold nanorods functionalized with a responsive polypeptide

can be used for reversible end-to-end self-assembly. It was shown that by simply altering the pH of the system, the gold nanorods could be cycled between an assembled state and disassembled state in a short amount of time. This reversible assembly was achieved by exploiting the conformational change of a PLGA biopolymer. PLGA leads to hydrophobic and dipole-dipole interactions when it exists in an α-helical conformation and mediates the end-to-end self-assembly of the gold nanorods. Upon changing the solution pH, the polypeptide changes its conformation to a random coil and leads to a reversal of the self-assembly. In addition to features such as simplicity of surface modification and rapid assembly, use of stimuli-responsive SSPLGA polymer also allows multiple cycles of assembly and dispersion. Extension to other biopolymers and exploitation of other secondary and tertiary conformations can lead to innovative and useful principles for directed self-organization of nanorods and nanoparticles.

Due to the vast flexibility in controlling the surface chemistry of these particles through functionalization, as shown throughout this work, the use of gold nanorods as building blocks in the development of more complex nanostructures and devices[3, 5-15] has significant potential. With the discovery of numerous applications in optics, electronics, catalysis and sensors[1-5], it is clear that the ability to control the self-assembly of gold nanorods and other nanoparticles will continue to be a matter of great importance for the development of future technology which operates on the micro and nano scale.

5.2 Future Work

Use of macro-cyclic compounds such as resorcinarenes can provide another useful strategy for directing the self-assembly of gold nanorods via multi-site interactions. One such compound is currently under investigation in collaboration with Bisht and Alazemi in the Department of Chemistry at USF. These resorcinarenes derivatives are modified with alkyl groups containing a sulfide on both sides of the bowl as shown in Figure 5.1 and Figure 5.2. It is proposed that these molecules can be used to drive the assembly of gold nanorods in a similar manner to the hexanedithiol explored in Chapter Three. The difference will provide a larger molecular footprint on the ends of the gold nanorod and could potentially lead to improvements in one-dimensional assembly.

Preliminary experiments in self-assembling these compounds onto planar gold surfaces have been performed in two different solvents to gain insight into the self-assembly process. Gold films were deposited by thermal evaporation on glass slides to a thickness of 100 nm. Onto these films, the modified resorcinarenes were self-assembled and examined by PM-IRRAS spectroscopy. To contrast the assembly of the resorcinarenes, monolayers of a single long-chain molecule such as Hexadecanethiol ($CH_3(CH_2)_{15}SH$) were also assembled. The absorbance of methyl groups and methylenes moieties can be seen in the 2800-3000cm^{-1} region[91] of the reflection IR spectra shown in Figure 5.3. The absorbance of the methylene groups is lessened in the case of the resorcinarenes as the lengths of the alkyl chains are shorter than those in the

hexadecanethiol. Also, the peaks for the assembly of the hexadecanethiol mono-layers are shifted to higher wave numbers. This shift is indicative of well-ordered, pseudo-crystalline monolayers where the alkyl chains have strong interactions with their neighboring chains[91]. In the region near 1500cm-1 region (not shown, preliminary results show a weak peak indicative of C=C stretching in the aromatic ring[91] of the resorcinarenes. Also, the intensity of the C-H stretching which is found in this region is significantly reduced in the case of the resorcinarene monolayers when compared to hexadecanethiol monolayers.

Understanding and establishing the self-assembly behavior of resorcinarene derivatives on gold surfaces will be a first step in utilizing these novel macro-cycles for modifying the gold nanorods and directing their assembly into organized structures.

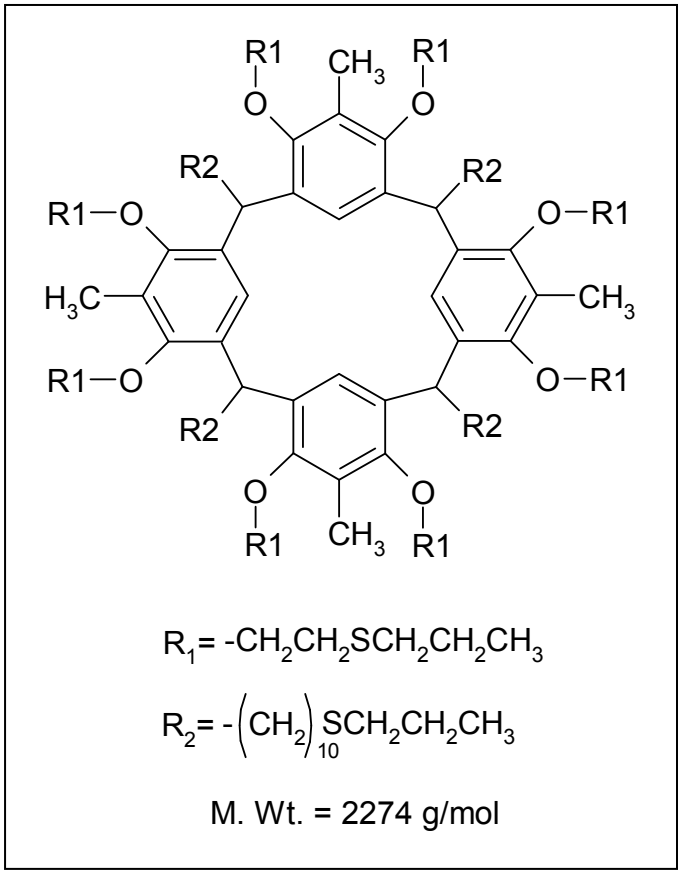

Figure 5.1: Chemical Structure of Sulfide Modified Resorcinarene Molecule

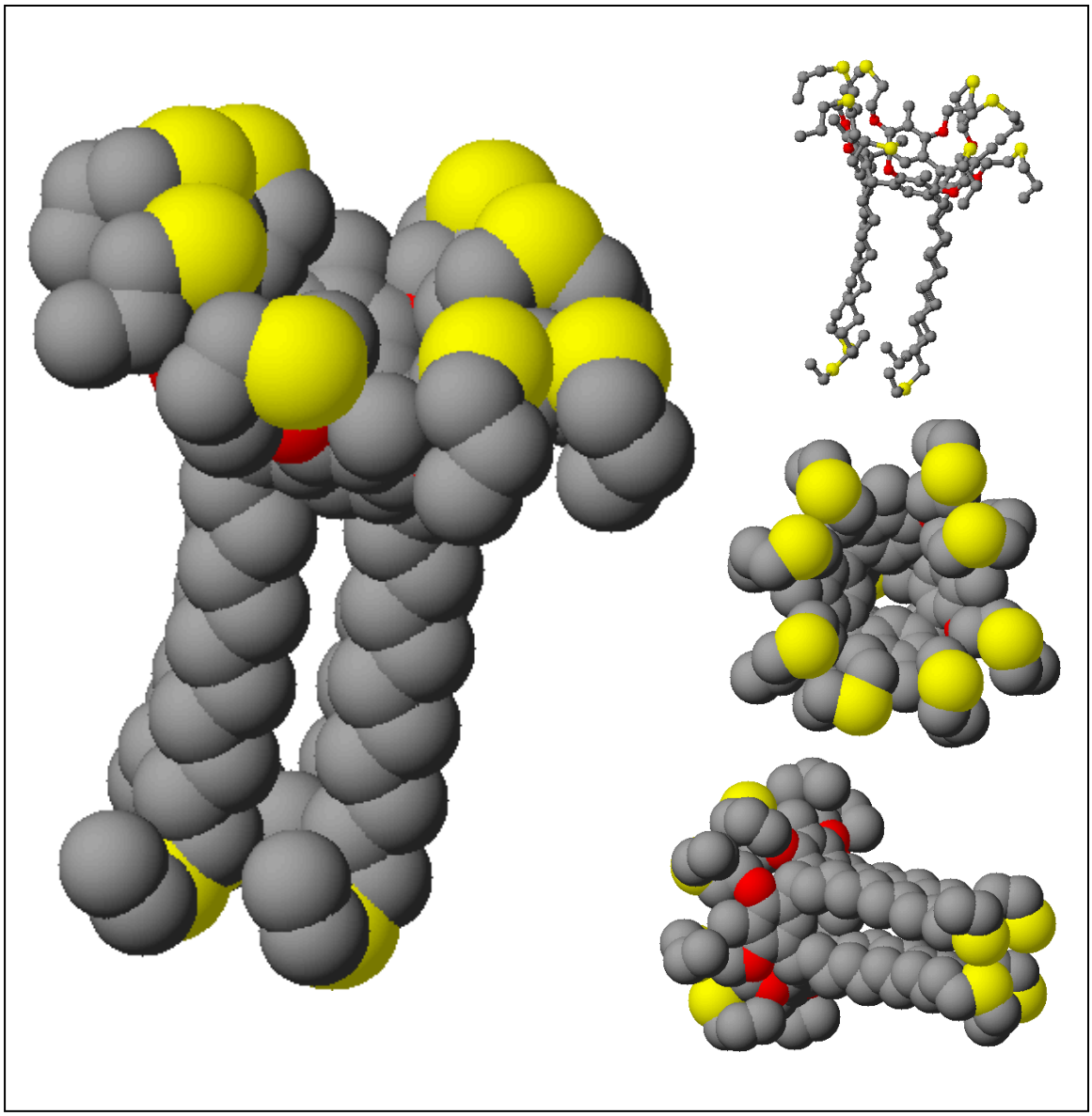

Figure 5.2: 3-D Schematic of Sulfide Modified Resorcinarene Molecule

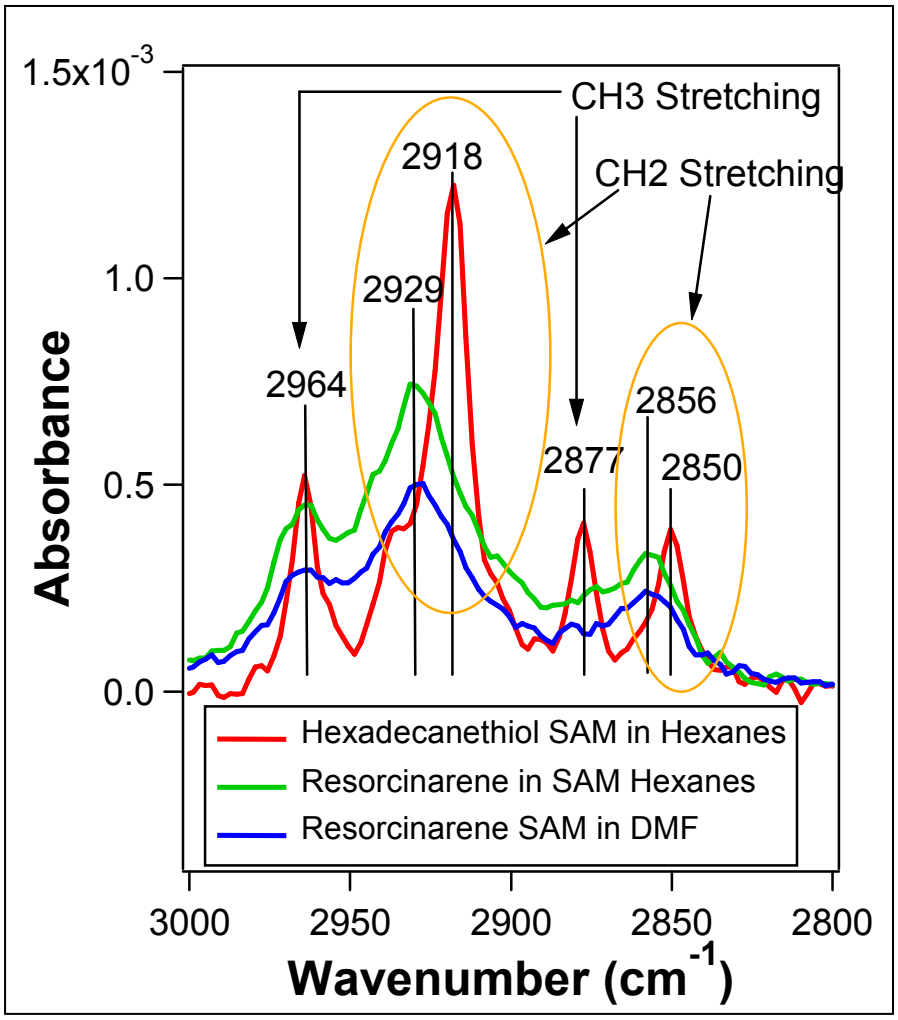

Figure 5.3: Reflection Absorption IR Spectra (C-H stretching region) of Sulfide Modified Resorcinarene Molecules Self-Assembled onto a Gold Film from DMF or Hexane Compared to SAMs of Hexadecanethiol

REFERENCES

1. M. Brust; C. J. Kiely, *Colloids and Surfaces, A: Physicochemical and Engineering Aspects* 2002, 202, (2-3), 175-186.

2. G. Hodes, *Advanced Materials* 2007, 19, (5), 639-655.

3. S. Mann; W. Shenton; M. Li; S. Connolly; D. Fitzmaurice, *Advanced Materials* 2000, 12, (2), 147-150.

4. P. Mulvaney, *Nanoscale Materials in Chemistry* 2001, 121-167.

5. V. M. Rotello, *Materials Today* 2001, 4, (6), 24-29.

6. Z. M. Fresco; J. M. J. Frechet, *Journal of the American Chemical Society* 2005, 127, (23), 8302-8303.

7. H. Huang; J. N. Anker; K. Wang; R. Kopelman, *Journal of Physical Chemistry B* 2006, 110, (40), 19929-19934.

8. B. P. Khanal; E. R. Zubarev, *Angewandte Chemie, International Edition* 2007, 46, (13), 2195-2198.

9. N. Malikova; I. Pastoriza-Santos; M. Schierhorn; N. A. Kotov; L. M. Liz-Marzan, *Langmuir* 2002, 18, (9), 3694-3697.

10. N. A. Melosh; A. Boukai; F. Diana; B. Gerardot; A. Badolato; P. M. Petroff; J. R. Heath, *Science* 2003, 300, (5616), 112-115.

11. B. A. Parviz; D. Ryan; G. M. Whitesides, *IEEE Transactions on Advanced Packaging* 2003, 26, (3), 233-241.

12. L. Samuelson, *Materials Today* 2003, 6, (10), 22-31.

13. M. Schmittel; V. Kalsani, *Topics in Current Chemistry* 2005, 245, (Functional Molecular Nanostructures), 1-53.

14. W. Shenton; S. A. Davis; S. Mann, *Advanced Materials* 1999, 11, (6), 449-452.

15. J. J. Storhoff; C. A. Mirkin, *Chemical Reviews* 1999, 99, (7), 1849-1862.

16. M. M. Alvarez; J. T. Khoury; T. G. Schaaff; M. N. Shafigullin; I. Vezmar; R. L. Whetten, *Journal of Physical Chemistry B* 1997, 101, (19), 3706-3712.

17. J. Gao; C. M. Bender; C. J. Murphy, *Langmuir* 2003, 19, (21), 9065-9070.

18. A. Gole; C. J. Murphy, *Chemistry of Materials* 2005, 17, (6), 1325-1330.

19. N. R. Jana, *Small* 2005, 1, (8-9), 875-882.

20. C. J. Johnson; E. Dujardin; S. A. Davis; C. J. Murphy; S. Mann, *Journal of Materials Chemistry* 2002, 12, (6), 1765-1770.

21. C. J. Murphy; T. K. Sau; A. M. Gole; C. J. Orendorff; J. Gao; L. Gou; S. E. Hunyadi; T. Li, *Journal of Physical Chemistry B* 2005, 109, (29), 13857-13870.

22. C. J. Orendorff; C. J. Murphy, *Journal of Physical Chemistry B* 2006, 110, (9), 3990-3994.

23. Y.-Y. Yu; S.-S. Chang; C.-L. Lee; C. R. C. Wang, *Journal of Physical Chemistry B* 1997, 101, (34), 6661-6664.

24. P. Zijlstra; C. Bullen; J. W. M. Chon; M. Gu, *Journal of Physical Chemistry B* 2006, 110, (39), 19315-19318.

25. A. Agarwal; S. W. Huang; M. O'Donnell; K. C. Day; M. Day; N. Kotov; S. Ashkenazi, *Journal of Applied Physics* 2007, 102, (6), 064701/1-064701/4.

26. G. K. Darbha; U. S. Rai; A. K. Singh; P. C. Ray, *Chemistry--A European Journal* 2008, 14, (13), 3896-3903.

27. C. M. Niemeyer, *Angewandte Chemie, International Edition* 2001, 40, (22), 4128-4158.

28. M. Rex; F. E. Hernandez; A. D. Campiglia, *Analytical Chemistry* 2006, 78, (2), 445-451.

29. P. K. Sudeep; S. T. S. Joseph; K. G. Thomas, *Journal of the American Chemical Society* 2005, 127, (18), 6516-6517.

30. C. Yu; J. Irudayaraj, *Analytical Chemistry* 2007, 79, (2), 572-579.

31. S. A. Maier; M. L. Brongersma; P. G. Kik; H. A. Atwater, *Physical Review B: Condensed Matter and Materials Physics* 2002, 65, (19), 193408/1-193408/4.

32. S. A. Maier; P. G. Kik; H. A. Atwater; S. Meltzer; E. Harel; B. E. Koel; A. A. G. Requicha, *Nature Materials* 2003, 2, (4), 229-232.

33. C. J. Murphy; A. M. Gole; S. E. Hunyadi; C. J. Orendorff, *Inorganic Chemistry* 2006, 45, (19), 7544-7554.

34. C. J. Murphy; A. M. Gole; S. E. Hunyadi; J. W. Stone; P. N. Sisco; A. Alkilany; B. E. Kinard; P. Hankins, *Chemical Communications* 2008, (5), 544-557.

35. P. Mulvaney, *Langmuir* 1996, 12, (3), 788-800.

36. S. Underwood; P. Mulvaney, *Langmuir* 1994, 10, (10), 3427-30.

37. B. Nikoobakht; M. A. El-Sayed, *Chemistry of Materials* 2003, 15, (10), 1957-1962.

38. S. Eustis; M. El-Sayed, *Journal of Physical Chemistry B* 2005, 109, (34), 16350-16356.

39. C.-Z. Li; K. B. Male; S. Hrapovic; J. H. T. Luong, *Chemical Communications* 2005, (31), 3924-3926.

40. M. B. Mohamed; V. Volkov; S. Link; M. A. El-Sayed, *Chemical Physics Letters* 2000, 317, (6), 517-523.

41. J. Nappa; G. Revillod; J.-P. Abid; I. Russier-Antoine; C. Jonin; E. Benichou; H. Girault Hubert; F. Brevet Pierre, *Faraday Discussions* 2004, 125, 145-56.

42. C. A. Foss, Jr.; G. L. Hornyak; J. A. Stockert; C. R. Martin, *Journal of Physical Chemistry* 1992, 96, (19), 7497-9.

43. C. R. Martin, *Science* 1994, 266, (5193), 1961-6.

44. C. R. Martin, *Chemistry of Materials* 1996, 8, (8), 1739-1746.

45. V. M. Cepak; C. R. Martin, *Journal of Physical Chemistry B* 1998, 102, (49), 9985-9990.

46. J. C. Hulteen; C. R. Martin, *Journal of Materials Chemistry* 1997, 7, (7), 1075-1087.

47. S.-S. Chang; C.-W. Shih; C.-D. Chen; W.-C. Lai; C. R. C. Wang, *Langmuir* 1999, 15, (3), 701-709.

48. M. Toernblom; U. Henriksson, *Journal of Physical Chemistry B* 1997, 101, (31), 6028-6035.

49. K. R. Brown; D. G. Walter; M. J. Natan, *Chemistry of Materials* 2000, 12, (2), 306-313.

50. B. Nikoobakht; M. A. El-Sayed, *Langmuir* 2001, 17, (20), 6368-6374.

51. B. M. I. van der Zande; M. R. Boehmer; L. G. J. Fokkink; C. Schoenenberger, *Langmuir* 2000, 16, (2), 451-458.

52. S. Vial; I. Pastoriza-Santos; J. Perez-Juste; L. M. Liz-Marzan, *Langmuir* 2007, 23, (8), 4606-4611.

53. J. Perez-Juste; B. Rodriguez-Gonzalez; P. Mulvaney; L. M. Liz-Marzan, *Advanced Functional Materials* 2005, 15, (7), 1065-1071.

54. H. Groenbeck; A. Curioni; W. Andreoni, *Journal of the American Chemical Society* 2000, 122, (16), 3839-3842.

55. L. A. Porter, Jr.; D. Ji; S. L. Westcott; M. Graupe; R. S. Czernuszewicz; N. J. Halas; T. R. Lee, *Langmuir* 1998, 14, (26), 7378-7386.

56. Y.-S. Shon; C. Mazzitelli; R. W. Murray, *Langmuir* 2001, 17, (25), 7735-7741.

57. K. K. Caswell; J. N. Wilson; U. H. F. Bunz; C. J. Murphy, *Journal of the American Chemical Society* 2003, 125, (46), 13914-13915.

58. J.-Y. Chang; H. Wu; H. Chen; Y.-C. Ling; W. Tan, *Chemical Communications* 2005, (8), 1092-1094.

59. X. Hu; W. Cheng; T. Wang; E. Wang; S. Dong, *Nanotechnology* 2005, 16, (10), 2164-2169.

60. S. T. S. Joseph; B. I. Ipe; P. Pramod; K. G. Thomas, *Journal of Physical Chemistry B* 2006, 110, (1), 150-157.

61. K. G. Thomas; S. Barazzouk; B. I. Ipe; S. T. S. Joseph; P. V. Kamat, *Journal of Physical Chemistry B* 2004, 108, (35), 13066-13068.

62. Z. L. Wang; M. B. Mohamed; S. Link; M. A. El-Sayed, *Surface Science* 1999, 440, (1-2), L809-L814.

63. S. Zhang; X. Kou; Z. Yang; Q. Shi; G. D. Stucky; L. Sun; J. Wang; C. Yan, *Chemical Communications* 2007, (18), 1816-1818.

64. N. J. Durr; T. Larson; D. K. Smith; B. A. Korgel; K. Sokolov; A. Ben-Yakar, *Nano Letters* 2007, 7, (4), 941-945.

65. P. A. Smith; C. D. Nordquist; T. N. Jackson; T. S. Mayer; B. R. Martin; J. Mbindyo; T. E. Mallouk, *Applied Physics Letters* 2000, 77, (9), 1399-1401.

66. Y. Dirix; C. Bastiaansen; W. Caseri; P. Smith, *Advanced Materials* 1999, 11, (3), 223-227.

67. M. S. Chen; D. W. Goodman, *Science* 2004, 306, (5694), 252-255.

68. M. Haruta, *Gold Bulletin* 2004, 37, (1-2), 27-36.

69. X. Huang; I. H. El-Sayed; W. Qian; M. A. El-Sayed, *Journal of the American Chemical Society* 2006, 128, (6), 2115-2120.

70. T. B. Huff; L. Tong; Y. Zhao; M. N. Hansen; J.-X. Cheng; A. Wei, *Nanomedicine* 2007, 2, (1), 125-132.

71. H. Takahashi; T. Niidome; A. Nariai; Y. Niidome; S. Yamada, *Chemistry Letters* 2006, 35, (5), 500-501.

72. P. L. Gai; M. A. Harmer, *Nano Letters* 2002, 2, (7), 771-774.

73. C. Wang; Z. Ma; T. Wang; Z. Su, *Advanced Functional Materials* 2006, 16, (13), 1673-1678.

74. I. Pastoriza-Santos; J. Perez-Juste; L. M. Liz-Marzan, *Chemistry of Materials* 2006, 18, (10), 2465-2467.

75. P. K. Jain; K. S. Lee; I. H. El-Sayed; M. A. El-Sayed, *Journal of Physical Chemistry B* 2006, 110, (14), 7238-7248.

76. I. Pastoriza-Santos; D. Gomez; J. Perez-Juste; L. M. Liz-Marzan; P. Mulvaney, *Physical Chemistry Chemical Physics* 2004, 6, (21), 5056-5060.

77. E. Dujardin; S. Mann; L.-B. Hsin; C. R. C. Wang, *Chemical Communications* 2001, (14), 1264-1265.

78. Z. Nie; D. Fava; E. Kumacheva; S. Zou; G. C. Walker; M. Rubinstein, *Nature Materials* 2007, 6, (8), 609-614.

79. P. K. Jain; S. Eustis; M. A. El-Sayed, *Journal of Physical Chemistry B* 2006, 110, (37), 18243-18253.

80. A. Ortega; J. Garcia de la Torre, *Journal of Chemical Physics* 2003, 119, (18), 9914-9919.

81. J. Rodriguez-Fernandez; J. Perez-Juste; L. M. Liz-Marzan; P. R. Lang, *Journal of Physical Chemistry C* 2007, 111, (13), 5020-5025.

82. K. Mitamura; T. Imae; N. Saito; O. Takai, *Journal of Physical Chemistry B* 2007, 111, (30), 8891-8898.

83. J. Perez-Juste; M. A. Correa-Duarte; L. M. Liz-Marzan, *Applied Surface Science* 2004, 226, (1-3), 137-143.

84. L. M. Liz-Marzan; M. Giersig; P. Mulvaney, *Langmuir* 1996, 12, (18), 4329-4335.

85. V. I. Boev; J. Perez-Juste; I. Pastoriza-Santos; C. J. R. Silva; M. De Gomes; L. M. Liz-Marzan, *Langmuir* 2004, 20, (23), 10268-10272.

86. S. O. Obare; N. R. Jana; C. J. Murphy, *Nano Letters* 2001, 1, (11), 601-603.

87. P. A. Buining; L. M. Liz-Marzan; A. P. Philipse, *Journal of Colloid and Interface Science* 1996, 179, (1), 318-21.

88. J.-Y. Shim; V. K. Gupta, *Journal of Colloid and Interface Science* 2007, 316, (2), 977-983.

89. A. J. Williams; V. K. Gupta, *Journal of Physical Chemistry B* 2001, 105, (22), 5223-5230.

90. M. Gluodenis; C. A. Foss, Jr., *Journal of Physical Chemistry B* 2002, 106, (37), 9484-9489.

91. R. M. Silverstein; G. C. Bassler; T. C. Morrill, *Spectrometric Identification of Organic Compounds*. 4th ed.; John Wiley & Sons: New York, 1981; p 442.